Universidade de Aveiro
2023

João Miguel Gomes Tomás

# FOSFORILAÇÃO DA PROTEÍNA KSR1 INDUZIDA POR ZINCO EM CÉLULAS DE CANCRO DA PRÓSTATA

# ZINC INDUCED PHOSPHORYLATION OF KSR1 PROTEIN IN PROSTATE CANCER CELLS

**Universidade de Aveiro**
**2023**

**João Miguel Gomes Tomás**

# FOSFORILAÇÃO DA PROTEÍNA KSR1 INDUZIDA POR ZINCO EM CÉLULAS DE CANCRO DA PRÓSTATA

# ZINC INDUCED PHOSPHORYLATION OF KSR1 PROTEIN IN PROSTATE CANCER CELLS

Dissertação apresentada à Universidade de Aveiro para cumprimento dos requisitos necessários à obtenção do grau de Mestre em Biologia Molecular e Celular, realizada sob a orientação científica do Doutor Jürgen Müller, Reader em Farmácia da School of Pharmacy da University of Bradford e do Doutor Artur Jorge da Costa Peixoto Alves, Professor Associado com agregação do Departamento de Biologia da Universidade de Aveiro

**o júri**

| | |
|---|---|
| presidente | Professora Doutora Susana Patrícia Mendes Loureiro<br>Professor Associado C/ Agregação, Universidade de Aveiro |
| vogais | Professora Doutora Margarida Sâncio da Cruz Fardilha<br>Professor Auxiliar C/ Agregação, Universidade de Aveiro |
| | Doutor Jürgen Müller<br>Reader, University Of Bradford |

**agradecimentos**

Durante muito tempo considerei que o sucesso era algo que dependia de mim e do meu esforço dedicação e trabalho, e que o mérito era meu e meu apenas. Esta jornada ensinou-me que o meu sucesso depende de muitas pessoas que me rodeiam, que me moldam, ensinam, apoiam.
Sobretudo ensinou-me que o mérito é algo que se partilha com quem ajudou a criar o sucesso.

Assim tenho de agradecer a quem foi crucial a fazer-me chegar onde estou.

À minha família, aos meus pais, à minha irmã Adriana e aos meus irmãos Alex e André eu agradeço profundamente pelo apoio desde o berço, por me ajudarem a construir a minha identidade e por me moldarem a ter uma mentalidade de esforço, trabalho e ambição. Por proporcionarem o sonho e estarem presentes desde o início até ao fim.

Aos famosos Papis, que nunca pude prescindir deles, que me fizeram sentir vivo, sentir que quero que o amanhã chegue, que se tudo cair eu tenho onde me agarrar.

Às minhas totós de Aveiro que sem elas nem o primeiro ano de mestrado tinha concluído, e por me fazerem sentir sempre que Aveiro é casa.

Às meninas da Giulia, Carolina e Enrica que transformaram Bradford numa cidade bonita, as minhas únicas companhias, primeiro porque não havia mais, segundo porque não queria outras.

Ao Professor Artur por aceitar ser o meu orientador, me ajudar no lançamento da minha carreira e principalmente por ter feito esta oportunidade acontecer.

Por fim ao Doutor Jürgen Müller que quebrou as barreiras de orientador e foi também um amigo, por me motivar todos os dias, por me fazer acreditar que nenhum desafio é grande demais, e principalmente por ser a pessoa a quem eu posso recorrer quando a família está longe. Que o nosso trabalho continue por muito tempo.

Um obrigado a todos!

**palavras-chave** KSR1, Zinc, Prostate cancer, Signalling Pathway, ERK 1/2, MAPK

**resumo**

Cancro da próstata é uma das causas mais comuns de morte em homens e as opções de tratamento para cancro da próstata avançado são limitadas. O Zinco é um ião vital que desempenha um papel crucial na fisiologia da próstata. Zinco encontra-se particularmente concentrado em células da próstata normais, sendo maioritariamente usado para produção de citrato. Por outro lado, o Zinco encontra-se muito reduzido em cancro da próstata, o que leva a um estado metabólico energeticamente mais eficiente. Curiosamente, o Zinco tem sido associado a afetar negativamente a via de sinalização MAPK. Neste estudo, as linhas celulares de cancro da próstata DU-145 e PC-3 foram testadas com ZnSO4 para avaliar a fosforilação de KSR1, uma proteína esqueleto da via MAPK/ERK 1/2. Os nossos resultados revelaram que apenas a linha celular DU-145 transfectada com um plasmídeo KSR1 apresentou níveis detetáveis de KSR1. Para ultrapassar a diminuta absorção de zinco pelas linhas celulares de cancro da próstata, as células transformadas K1-4 foram utilizadas para provar que KSR1 modula a atividade da ERK 1/2. Este papel da proteína KSR1 foi confirmada por inibidores de MEK e KSR1 que demonstraram que a inibição de KSR1 resulta numa ativação reduzida da ERK 1/2. Isto correlaciona com a hipótese de que a fosforilação da proteína KSR1 induzida por Zinco leva a uma menor atividade da ERK 1/2. Assim a KSR1 pode ser considerada como um novo alvo válido para o desenvolvimento de terapias de cancro da próstata.

**Keywords** KSR1, Zinc, Prostate cancer, Signalling Pathway, ERK 1/2, MAPK

**Abstract**

Prostate cancer is one of the most common causes of cancer death in men and the treatment options are limited for advanced prostate cancer. Zinc is a vital metal ion that plays a crucial role in prostate physiology. Zinc is particularly concentrated in normal prostate cells, being mainly used for citrate secretion. On the other hand, Zinc levels are heavily reduced in prostate cancer, which lead to a more energy-efficient metabolic state. Interestingly, Zinc has also been shown to negatively affect MAPK signalling. In this study, DU-145 and PC-3 prostate cancer cell lines were tested with ZnSO4 for the assessment of the phosphorylation of KSR1, a scaffold protein of the MAPK/ERK 1/2 pathway. Our findings revealed that only the DU-145 cell line transfected with KSR1 plasmid presented detectable phosphorylation levels of KSR1. To overcome the scarce uptake of Zinc by prostate cancer cell lines, the transformed K1-4 cells were used to prove the modulation of ERK 1/2 activity by KSR1. This role of KSR1 was confirmed by MEK and KSR1 inhibitors that demonstrated that the inhibition of KSR1 results in diminished ERK 1/2 activation. This correlates with the hypothesis that the Zinc-induced phosphorylation of KSR1 leads to lower ERK 1/2 activity. KSR1 can be therefore considered as a new valid target for the development of prostate cancer therapies.

# List of Figures

# List of Tables

# Table of Content

# 1. Introduction

## 1.1. Prostate and prostate cancer (anatomy and disease development)

### 1.1.1. Prostate gland

Prostate gland is a reproductive organ located caudal to the bladder and cranial to the penis, below the internal urethral orifice and around the beginning of the urethra. It is a walnut-sized exocrine gland with the primary function of secreting seminal fluid that aids the motility and nourishment of sperm during and after ejaculation and its alkalinity protects the sperm in the acidic environment of the vagina [1–4].

This gland is anatomically divided in four zones: central, transition, fibromuscular and peripheral zones. Prostate zones have different embryologic origins, therefore susceptibility to carcinogenesis vary across the zones. The central zone has a very low rate of prostate cancer incidence. Contrarily, the peripheral zone is where 75% of prostate cancers develop. Given the proximity of the prostate gland to the rectum, the peripheral zone located in the posterior part of the gland is most prominent on Digital Rectum Examination (DRE) [3–6].

Despite similarities between the peripheral zone and transition zone embryologic origins, only 25% of prostate cancers occur in the latter, which might be due to differences in the stromal cells in these zones.

Transition zone stroma contains a higher proportion of fibromuscular components (smooth muscle cells, fibroblasts, and collagen fibres), which are responsible for maintaining the structure and function of the prostate gland. This fibromuscular stroma of the transition zone has been associated with the development of Benign Prostatic Hyperplasia (BPH) and it is conductive for cancer development.

Contrarily, the Peripheral Zone has a different stromal composition, with less fibromuscular components and a high proportion of glandular epithelial cells. These cells are more susceptible to malignant transformation hence the increased incidence of cancer in this zone [3–5,7].

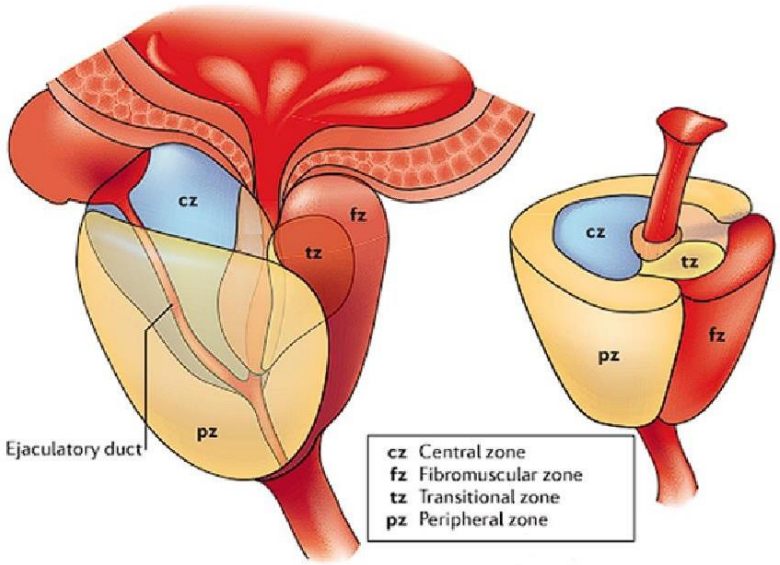


*Figure 1. Prostate gland zones - lateral view and overview (adapted from Rebello et. al)*

The prostate gland is mainly formed by epithelial cells (columnar luminal, basal and neuroendocrine) and stromal cells. The epithelial cells constitute the ducts and acini (oval-shaped structure that produces and secretes prostatic fluid). A single layer of basal cells surrounds a layer of columnar luminal secretory cells, both intercalated by rare neuroendocrine cells with prostate neuron-like functions. The ducts and acini (glands) are embedded in stroma (connective tissue made of stromal cells) which provides structural support and a supporting environment [5,6,8,9].

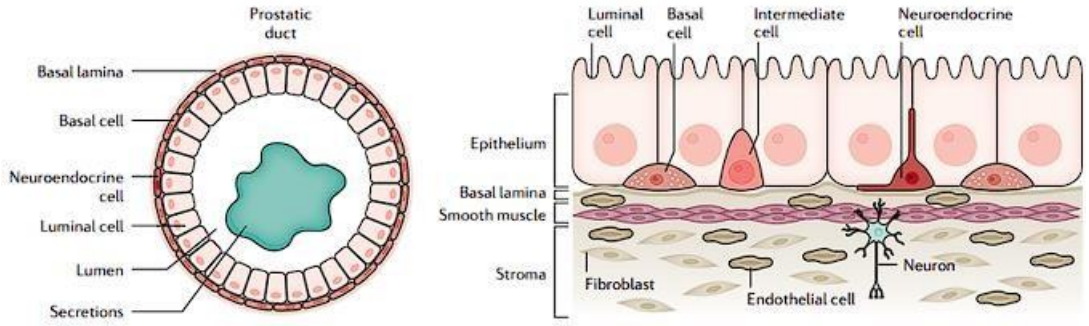


*Figure 2. Representation of epithelial cells on prostatic duct (left) and organization of epithelial cells and stroma (right) ((adapted from Rebello et. al)*

### 1.1.2. Prostate cancer

Prostate cancer is the most common cancer in men aged +45 years old worldwide and its incidence and mortality are expected to increase in the following years[10]. It is widely considered as an elderly disease with most of the diagnosed cases reported on men aged more than 65 years old and aging being the leading risk factor for this disease [1,5,11,12].

While early-stage prostate cancer is widely treatable with a survival rate around 98.9% to 100% in a 5-year time since diagnosis, advanced prostate cancer is much more difficult to treat and has a lower survival rate of 28% for the same period. As such, early detection and treatment of prostate cancer is crucial to increase survival and prevent advanced prostate cancer [13,14].

### 1.1.3. Epithelial cells and prostate cancer

Prostate cancer is referred to as an adenocarcinoma, this is due to more than 95% of prostate cancer originating in epithelium cells [2,7]. In both normal and cancerous prostate tissue, epithelial cells express high levels of the androgen receptor (AR), which is encoded by the AR gene [5,15]. As such, the prostate is an androgen-dependent organ regulated by the interaction of AR with androgens. These are crucial for prostate development, morphology, and normal function; in early stages of development, they "act" as growth factors hence regulating cell proliferation and differentiation; in a mature prostate they guarantee maintenance and normal function of the prostatic tissue [16,17].
In the interaction with AR, androgens promote AR activation and translocation to the cell nucleus where it targets genes involved in various cellular processes, protein syntheses and growth factor secretion. However, androgens are also regarded as drivers for tumorigenesis. In early stages of tumorigenesis, the prostate cancer cells depend on androgens for growth promotion and inhibition of apoptosis. With disease progression, genetic alterations enable cells to survive and proliferate within low androgen levels, thus becoming androgen-independent prostate cancer. At this stage the tumour becomes invasive, spreads to adjacent tissues and later metastasizes to distant organs [16,18].
Prostate Specific Antigen (PSA) is an enzyme produced in the prostate gland and it is also expressed by these epithelial cells, its function in the prostate is to help sperm mobility by liquefying the coagulated semen [19]. However, the PSA coding gene is regulated by AR and, in the context of prostate cancer, the activity of AR leads to an increase of the PSA coding gene expression resulting in high levels of PSA in the blood, this explains why PSA is used as a biomarker in the detection and diagnosis of prostate cancer [3,5,20].

### 1.1.4. Prostate cancer heterogeneity

Prostate cancer is a complex and heterogeneous disease diagnosed through tissue biopsy and histological evaluation [20–22]. It is stratified based on the Gleason score, which measures the aggressiveness of the cancer, and the stage. The Gleason score system assigns a grade to Prostate cancer based on the degree of differentiation, appearance, and architectural pattern of cells. This ranges from low-grade, well-differentiated tumors (low risk) to high-grade, poorly differentiated tumours (high risk). The Gleason score is one of the parameters used alongside the TNM system (Tumor, Node, Metastasis) for cancer staging. The general stages include localized, locally advanced, and metastatic prostate cancer [1,3,4,18,21,23].

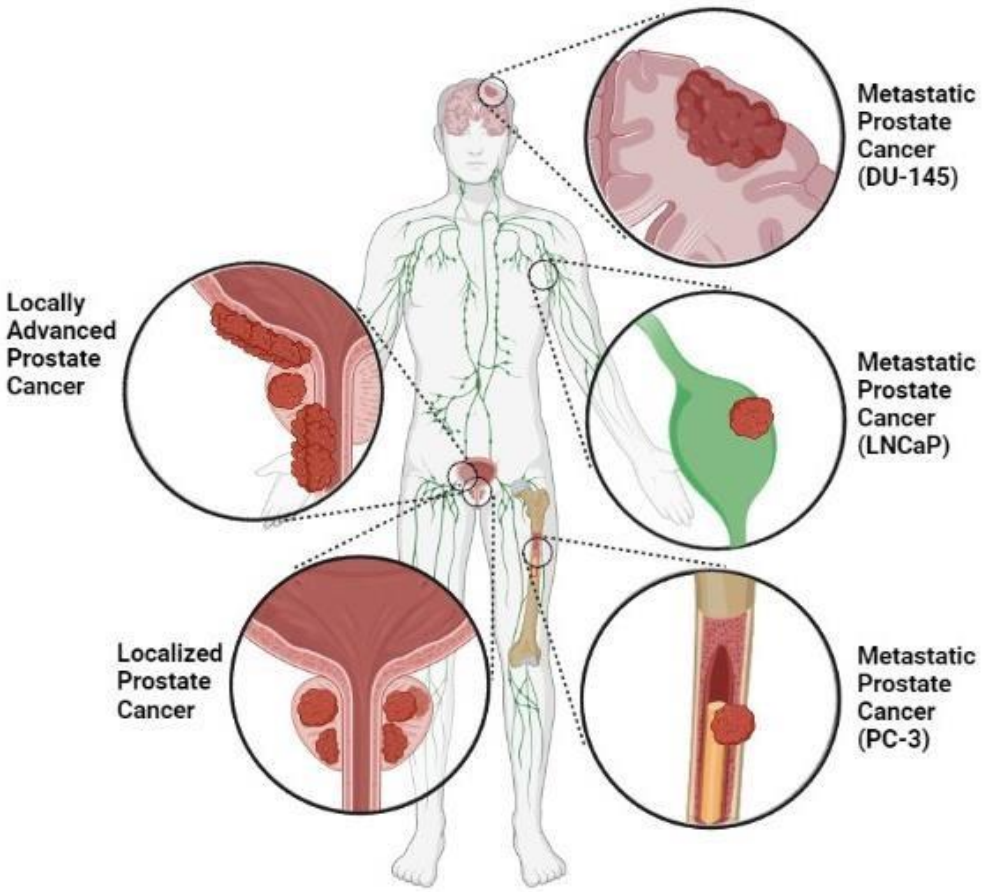


*Figure 3. Prostate cancer stages and common metastasis in the male body*

Localized Prostate Cancer (or early-stage Prostate cancer) is confined to the prostate gland without lymph nodes involvement or distant organ metastasis. This is a cancer with good prognosis as there are multiple curative options including radical prostatectomy, radiotherapy and cryotherapy, active surveillance is also adopted by many patients, thus resulting in high survival rates. High-risk localized Prostate cancer is frequently treated with radical prostatectomy with pelvic lymph node dissection which seems to reduce mortality [3,13,14,21,24,25].

Locally Advanced Prostate Cancer refers to tumours that have extended beyond the prostate gland capsule, infiltrating surrounding tissues, seminal vesicles, nearby organs (bladder, rectum, and pelvic wall), and pelvic lymph nodes. It is classified as T3 or T4 in the TNM staging system. The definition of locally advanced prostate cancer is not consensual, several institutions and studies include the pelvic lymph nodes involvement, but it is described as not having lymph nodes involvement [13,14,24–26].

Metastatic Prostate Cancer is described as the advanced stage of the disease when cancer cells have spread from the prostate to other parts of the body, commonly affecting lymph nodes, bones, and occasionally other organs like the lungs. Bone metastasis is the predominant form of metastasis observed in cases of metastatic prostate cancer and this preference to metastasize to the bones can be attributed to the favourable conditions offered

by the bone microenvironment, which creates an ideal setting for the growth and aggressive progression of tumour cells. Also, signalling molecules secreted by bone cells (bone-derived chemokines) attract and guide circulating prostate tumour cells to the bone, thus to the favourable microenvironment that promotes adhesion, survival, and growth of the tumour cells within the bone tissue[14,16,24,25].

Metastatic prostate cancer is broadly categorized in metastatic hormone-sensitive prostate cancer and metastatic castration-resistant prostate cancer. Androgen-dependent metastatic prostate cancer initially relies on androgen signalling for its growth and survival. Androgen receptor (AR) signalling, which is driven by testosterone, plays a significant role in the development and progression of androgen-dependent prostate cancer. This type of prostate cancer responds to androgen deprivation therapy (ADT), which aims to block or interrupt AR-dependent signalling pathways. ADT can effectively suppress the production or action of androgens, particularly testosterone, which inhibits the growth of androgen-dependent prostate cancer cells. However, over time, some prostate cancer cells may develop resistance to ADT, leading to the development of castration-resistant prostate cancer (CRPC), which is characterized by disease progression despite low levels of testosterone. Androgen-independent metastatic prostate cancer, on the other hand, refers to the advanced stage of prostate cancer that has spread to other parts of the body, including the bones, and is no longer responsive to androgen deprivation therapy (ADT). Despite initial responses to systemic treatment, this type of prostate cancer eventually becomes resistant to ADT, leading to disease progression [13,14,17,25].

Overall, the distinction between androgen-independent and androgen-dependent metastatic prostate cancer lies in their responsiveness to androgens and androgen deprivation therapy and the role of androgen signalling in their growth and progression; metastatic prostate cancer is associated with a higher risk of mortality and is considered uncurable.

### 1.1.5. Prostate Cancer Screening

Prostate-specific antigen testing, often combined with Digital Rectal Examination (DRE), is the most common approach for prostate cancer detection. However, both methods have limitations, with PSA testing potentially leading to over-diagnosis and unnecessary interventions and DRE leading to under-diagnosis as only the part of the prostate proximal to the rectum can be examined[1,2,5,12,17,20,22,23,27].

PSA testing is unable to distinguish between cancer types (indolent or aggressive) and its elevated levels not always correlate with prostate cancer (BPH presents elevated levels of PSA) which can result in over-treatment, affecting 20-50% of cases[2,3,20,22].

DRE, previously the primary screening tool, assesses the palpable part of the prostate and remains useful in identifying advanced cancer when PSA levels are normal (15% of cases). When patients have elevated PSA levels, abnormal DRE results, or both, an MRI is often employed to confirm the necessity of a biopsy and detect significant cancer confined within the prostate[1,3,5,23,28,29]. Most cases (91%) involve localized or early-stage prostate cancer,

which is generally curable, but a minority of cases are locally advanced or metastatic, considered incurable with a poorer prognosis[13,14,17].

## 1.2. MAPK/ERK1/2 Pathway

The MAPK/ERK 1/2 pathway is a signalling cascade involved in transmitting extracellular signals to the nucleus of a cell. It plays a crucial role in regulating various cellular processes, including cell growth, differentiation, proliferation, and survival. The MAPK/ERK 1/2 pathway also receives inputs from various stimuli including internal metabolic stress, DNA damage pathways, abnormal protein concentration, growth factors and communication from other cells, therefore it is crucial for cancer cell survival, proliferation, migration, invasion, and drug therapy resistance [30–34].

The successive events that activate the MAPK-ERK 1/2 pathway (Figure 4) start with the activation of a receptor (1) when a ligand (growth factor or cytokine) binds to a specific receptor on the cell surface, known as a Receptor Tyrosine Kinase (RTK). This binding leads to dimerization and autophosphorylation of the RTK, activating its intrinsic kinase activity. This leads to the recruitment and activation of Grb2 and SOS (2) where the phosphorylated RTK recruits an adaptor protein Grb2 (Growth Factor Receptor-Bound Protein 2), which binds to the phosphorylated RTK. Grb2 further recruits and activates SOS (Son of Sevenless), a guanine nucleotide exchange factor (GEF). The SOS promotes the exchange of GDP (guanosine diphosphate) for GTP (guanosine triphosphate) on the small GTPase protein called Ras. This causes Ras to switch from an inactive (Ras-GDP) to an active (Ras-GTP) state (3), hence becoming active. Active Ras-GTP binds to and activates Raf (Rapidly Accelerated Fibrosarcoma), a serine/threonine kinase, leading to the phosphorylation and activation of Raf (4). The activation of Raf starts a phosphorylation cascade (5) when Raf phosphorylates and activates MEK1/2, also known as MAPKK. MEK, in turn, phosphorylates and activates ERK 1/2 (Extracellular Signal-Regulated Kinase 1/2), also known as MAPK. In resting cells, the constituents of the ERK 1/2 module are located in the cytoplasm, upon stimulation, MEK anchors ERK in the cytoplasm before phosphorylating ERK 1/2. Once activated, ERK 1/2 dimerizes and translocates to the nucleus (6) resulting in its accumulation; while the mechanisms behind its accumulation in the nucleus are not fully understood, the phosphorylation of the nuclear translocation sequence (NTS) in the kinase insert domain allows the interaction of ERK 1/2 with nuclear importing proteins, this mechanism regulates ERK 1/2 translocation to the nucleus through nuclear pores. The nuclear translocation allows ERK 1/2 to phosphorylate and activate various transcription factors and other nuclear targets, leading to changes in gene expression. The phosphorylation of transcription factors by ERK 1/2 regulates the expression of specific genes involved in cell growth, proliferation, survival, and differentiation. Additionally, ERK 1/2 phosphorylates a variety of cytoplasmic and nuclear proteins, affecting various cellular processes (7). The MAPK-ERK 1/2 pathway includes several negative feedback

mechanisms to control its activity (8). These feedback loops help maintain appropriate signalling levels and prevent excessive or prolonged activation [35,36].

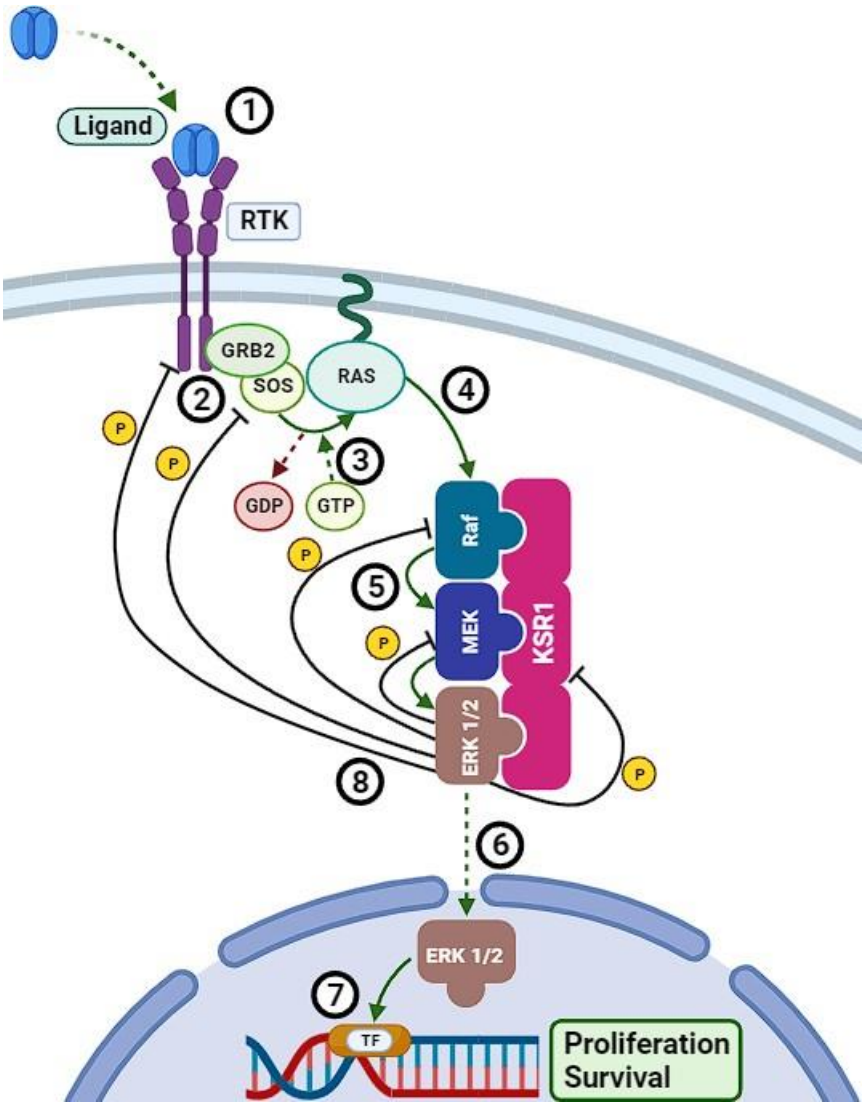


*Figure 4. MAPK/ERK 1/2 pathway activation upon extra-cellular stimulation, from ligand to nucleus*

### 1.2.1. ERK 1/2 Inhibition

It was showed that stopping MAPK/ERK 1/2 pathway inhibited cell proliferation and promoted apoptosis of a cell line of B cell lymphoma. Also, the use of MEK inhibitors to inhibit ERK 1/2 was also showed to prevent cells from progressing from G1 to S phase in colon cancer cells. Since ERK 1/2 regulates cell proliferation and its activation is necessary for cell progression from G1 to S phase, and growth of adherent cells, the use and development of MAPK/ERK 1/2 pathway inhibitors presents itself as a possible solution for cancer cell progression, differentiation, and its anti-apoptotic characteristics [30,32].

### 1.2.2. ERK 1/2 in cancer

The MAPK/ERK 1/2 pathway dysregulated hyperactivation, linked to activation mutations, has been related to neurological and development disorders, inflammation, and cancer. This excessive activation of the pathway is a prevalent oncogenic factor, and it is associated with cancer development, progression, and tumour cell migration. Also, the regulatory role of this pathway leads to cytoskeleton deformation and improves tumour invasion and metastasis[30].

The increased activation of this pathway has been linked to advanced prostate cancer, androgen independence and metastasis. Furthermore, the classical prostate cancer cell models (DU-145, PC-3 and LNCaP) were found to express lower levels of active Raf kinase inhibitors. It was demonstrated that ERK activation correlates with tumour malignancy and prostatic epithelial proliferation and cancer development; on the other hand, ERK inactivation was linked to androgen independent and inadequately differentiated metastatic prostate cancer. ERK is also known to phosphorylate proteins involved in cancer cell migration and tumour invasion by degrading the extracellular matrix[37].

## 1.3. Scaffold protein KSR1 in MAPK/ERK pathway

The Kinase Suppressor of Ras 1(KSR1) protein was initially introduced as part of a novel family of proteins – Kinase Suppressor of Ras family- which are structurally related to the Raf Kinase family. However, studies determined that KSR proteins present significant structural and functional differences. The KSR family (KSR1 and KSR2) were firstly observed in Drosophila (KSR1) and Caenorhabditis elegans (KSR1 and KSR2) as a modulator of the Ras Signalling pathway, a broader term for the signalling pathways initiated by the activation of Ras molecules, including the MAPK/ERK 1/2 pathway[38–41].

The role of KSR1 in the MAPK/ERK 1/2 pathway is complex and as suggested in its denomination, KSR1 was originally characterized as a protein kinase supported by several studies demonstrating a degree of intrinsic kinase activity. Such activity is still under scrutiny with many suggesting inconsistencies with the kinase domains of KSR1, even considering it a pseudo-kinase without kinase activity. This was supported by the lack of KSR1 substrates, and it was showed that mammalian KSR1 presents a mutation in the ATP binding site (arginine residue instead of lysine residue) that causes the inactivation of the kinase activity of this protein. It was also demonstrated that while KSR1 do not appears to have kinase activity, it interacts directly with kinase proteins such as MAPK and MEK, and both directly and indirectly with Raf-1 [40–44].

Hence it has been proposed that the main role of KSR1 in the MAPK/ERK 1/2 pathway is to act as a molecular scaffold protein enhancing the signalling cascade; upon growth factor

stimulation, KSR1 translocates to the plasma membrane, this allows the assembly of the Raf, MEK 1/2, ERK 1/2 module [35,38–40,42,43].
The regulatory role of KSR1 in the MAPK/ERK 1/2 pathway also seems to both promote and inhibit the signalling cascade. It was shown that increased KSR1 expression increases its interaction with Raf, MEK 1/2 and ERK 1/2, cell proliferation and ERK 1/2 signalling until the optimal levels of KSR1 are surpassed resulting in strong decrease in cell proliferation and ERK 1/2 signalling. This seems to be due to the KSR1 sequestrating the signalling constituents, thus dispersing the module components, and disrupting the signalling cascade [45].
The KSR1 protein is primarily located within the cytosol of resting or unstimulated cells. At this stage, MEK is colocalized with the KSR1 in the cytosol, forming an inactive KSR1/MEK complex. This results from the mediated phosphorylation of KSR1 by the kinase C-TAK1 (Cdc25C-associated kinase 1), which in turn creates a binding site for the 14-3-3 protein that constrains the complex in the cytosol.
This mechanism is inactivated upon growth factor stimulation by activated Ras that recruits Raf to the membrane and induces the dephosphorylation of KSR1 by PP2A, releasing 14-3-3, thus allowing its translocation to the cell membrane along with the bonded MEK. MAPK then binds to the activated complex which leads to the assembly of the Raf, MEK 1/2, ERK 1/2 module bringing all the component into close proximity, thus enhancing signalling transduction [45,46].

### 1.3.1. KSR1 in cancer

The role of KSR1 as a scaffold protein in the MAPK/ERK 1/2 pathway has been described in Ras-driven cancers (group of cancers that are characterized by mutations in genes that encode proteins involved in the Ras signalling pathway) as a promotor of Ras Signalling, enhancing the signalling pathway [39,45]. As such, KSR1 was found to be overexpressed in endometrial carcinoma, and has a significant role in the tumorigenesis of diverse cancers such as lung, colorectal and breast cancer [43,47].

However, in prostate cancer, this role is still not fully comprehended. While in other cancers the MAPK/ERK 1/2 pathway abnormal activity might result from mutations, in prostate cancer it is not related to mutations but to a constitutively activation of the pathway. The ERK 1/2 feedback phosphorylation is not enough to inhibit the upstream components including the KSR1 [39,42,45].
In normal prostate cells, KSR1 is inhibited after signalling transduction by mechanisms such as the ERK 1/2 feedback thus regulating signal strength and duration.
Conversely, prostate cancer cells appear to have lost this mechanism, therefore KSR1 remains active, allowing the Raf, MEK 1/2, ERK 1/2 module to stay assembled consequently promoting signalling [39,48].

### 1.3.2. Development of KSR1 inhibitors

The regulatory role of KSR1 in the MAPK/ERK 1/2 pathway caused interest in targeting this protein for therapy options. It was shown that the inhibition of KSR1 decreased tumour growth, inhibited metastases and even resulted in tumour regression.
A study involving a KSR1 inhibitor, the small molecule APS-2-79, demonstrated that it could stabilize KSR in its inactive state, however it could only bind effectively to KSR2 and not KSR1 which limits its efficacy.
But the limitations detected in this KSR1 inhibitor included significant efficacy only in Ras-mutated cancers and has limited cytotoxic effect.
This shows that while the APS-2-79 is, at this time, the only commercialized KSR inhibitor, it is not effective enough, thus revealing the importance and urgency of the development of better KSR1 inhibitors [45].

## 1.4. Negative feedback phosphorylation

A vital mechanism in the regulation of the MAPK/ERK pathway is the negative feedback phosphorylation. This mechanism ensures the precise control over the pathway by dampening and regulating the pathway activity thus preventing excessive signalling. This is achieved by downstream kinases that phosphorylate upstream components of the pathway, hence limiting their activity [35,49].

KSR1 is a key component of the pathway that undergoes negative feedback phosphorylation by ERK 1/2 in multiple residues to regulate its scaffolding function within the pathway. The ternary complex Raf, KSR1, MEK 1/2 is interrupted by the feedback phosphorylation directly affecting the cascade efficacy, this also results in the KSR1 translocating from the membrane to the cytosol diminishing the signal strength. KSR1 is also responsible for transporting MEK and active ERK 1/2 closer to Raf-1 during its translocation, thus assisting feedback phosphorylation of other pathway constituents [35,45,49].
The loss of the negative feedback phosphorylation mechanism in the MAPK/ERK 1/2 pathway can facilitate cancer progression and it is often associated with increased cell proliferation and survival. The aberrant function of this mechanism may result in excessive or insufficient pathway activation (which can be achieved with anti-cancer drugs) posing a challenge for therapies. Due to this, efforts have been made to understand the balance of feedback mechanism and pathway dysregulation in order to develop therapeutic strategies.

## 1.5. Zinc as a regulator of the activity of prostate cells

Zinc is essential in the human body as it is a cofactor for more than 300 enzymes involved in several cellular processes, such as cell proliferation and metabolism. This trace element is found to be highly concentrated in the prostate, with prostate tissues having a concentration ten times greater than the rest of the body tissues[50–52].

The prostate gland is dependent on zinc for its proper function. Secretory epithelial cells have a unique ability to accumulate zinc in their mitochondria which acts as an inhibitor of m-aconitase (an enzyme that catalyses the conversion of citrate to isocitrate in the Krebs cycle that generates ATP) hence preventing oxidation of citrate. Citrate is then a metabolic product of these cells used to secrete prostatic fluid.
The production of citrate is energetically expensive, however prostate cells prioritize citrate secretion, which yields few ATP molecules, over efficient ATP production [51–55].

The importance of zinc is also seen within malignancies associated with its deficiency. Low levels of zinc are linked to alterations in cellular processes including cell proliferation that can contribute to prostate cancer development and progression. In fact, it was demonstrated that zinc is able to inhibit invasive and migratory capacities of prostate cells, thus being characterized as a tumour suppressor. Added to this, decreased levels of zinc are necessary to allow invasion and metastasis. This decrease of high zinc concentrations results in reconstitution of m-aconitase activity and citrate oxidation, thus prostate cancer cells show efficient ATP production and cell proliferation [55,56].

The loss of zinc in prostate cancer cells is due to the loss of zinc transporters which function is to regulate proper zinc levels in the cell. This occurs during prostate cell transformation and results in decreased uptake of zinc. This loss of zinc accumulation in prostate cells is now seen as a hallmark for prostate cancer [56,57].

### 1.5.1. Modification of KSR1 phosphorylation by Zinc

Zinc also has a role in regulating KSR1 phosphorylation in mammalian tissue cells (HEK 293 cells), it was observed that elevated zinc levels have an effect on KSR1 phosphorylation and do not appear to be influenced by growth factors or phosphatase inhibitors suggesting a distinctive pathway [46].
It is still unknown how zinc induces KSR1 phosphorylation, however it was suggested that zinc may induce other kinases or regulatory components into affecting KSR1 phosphorylation [46].

## 1.6. Hypothesis and objectives

The hypothesis of this study is that Zinc induces KSR1 phosphorylation in prostate cancer cells, resulting in decreased ERK 1/2 activity.
As such, we set the following objectives for this study:

- Evaluating zinc induced phosphorylation in prostate cancer cells
- Evaluating the effect of KSR1 phosphorylation on ERK 1/2 activation
- Assessing MEK and KSR inhibitors on ERK 1/2 activity

# 2. Materials and Methods

## 2.1. Cell lines

The cell lines selected for this study were the classical Prostate cancer cell lines DU-145, PC-3 and LNCaP and the HEK-293 based cell line Flp-In™ 293 T-Rex - K1-4 (designated K1-4 in this study).

| Cell Line | Cell type | Androgen Sensitivity |
|---|---|---|
| **DU-145** | Adherent human epithelial prostate cancer cell line isolated from the brain of 69 years old male | Not sensitive to androgen |
| **PC-3** | Adherent human epithelial prostate cancer cell line isolated from bone metastasis of grade IV adenocarcinoma of a 62 years old male | Not sensitive to androgen |
| **LNCaP** | Adherent human epithelial prostate cancer cell line isolated from supraclavicular lymph node of a 50 years old male | Sensitive to androgen |
| **Flp-In™ 293 T-Rex - K1-4** | HEK293 derived cell line | N/A |

The Flp-In™ 293 T-Rex - K1-4 (K1-4) is a cell line previously constructed in the laboratory. It is based on the Flp-In ™ -293 (Invitrogen) cell line that has been stably transfected with KSR1 cloned into the plasmid pcDNA5/FRT/TO to provide tetracycline responsive expression of KSR1. KSR1 has also been tagged with the Glu-Glu epitope (M)EYMPME (2x) (amino acids 314 to 319 of the middle T antigen of mouse polymavirus) this permits the binding of an antibody to this specific tag allowing the analysis of the exogenous protein expression.

## Cell culture media

Cell culture was performed under sterile conditions in a safety cabinet. The media used is described in Table 1.

*Table 1. Cell culture media, composition and cell lines cultured.*

| Media | Composition | Cell lines used |
|---|---|---|
| **Dulbecco's Modified Eagle Medium – High Glucose D0819 (DMEM Full)** | Dulbecco's Modified Eagle Medium (DMEM) with 4,5g/L glucose, Sodium pyruvate, Sodium bicarbonate Supplemented with 10% (v/v) Fetal Bovine Serum (FBS) and 1% 100U/ml Penicillin/Streptomycin | **DU-145 PC-3 K1-4** |
| **Serum-free Dulbecco's Modified Eagle Medium – High Glucose D0819 (DMEM Starved)** | Dulbecco's Modified Eagle Medium (DMEM) with 4,5g/L glucose, Sodium pyruvate and Sodium bicarbonate | **DU-145 PC-3** |
| **Dulbecco's Modified Eagle Medium – High Glucose D0819 + Hygromycin/Blasticidin (DMEM+H/B Full)** | Dulbecco's Modified Eagle Medium (DMEM) with 4,5g/L glucose, Sodium pyruvate, Sodium bicarbonate Supplemented with 10% (v/v) Fetal Bovine Serum (FBS), 1% 100U/ml Penicillin/Streptomycin and 200µg/ml Hygromycin + 15µg/ml Blasticidin | **K1-4** |
| **Serum-free Dulbecco's Modified Eagle Medium D0819 + Hygromycin/Blasticidin (DMEM+H/B Starved)** | Dulbecco's Modified Eagle Medium (DMEM) with 4,5g/L glucose, Sodium pyruvate, Sodium bicarbonate Supplemented with 1% 100U/ml Penicillin/Streptomycin and 200µg/ml Hygromycin + 15µg/ml Blasticidin | **K1-4** |

## 2.2. Stock Cell Thawing

Stock cell lines (DU-145, PC-3 and K1-4) were cryopreserved in liquid nitrogen at -196ºC until needed for experiments. Cell thawing was executed by placing the cryovial in a 37ºC water bath until cells reached liquid state (2-3minutes) and were transferred to T75 flask with 12ml DMEM Full media.

## 2.3. Cell Maintenance

The cell lines were cultured in DMEM Full media and incubated at 37ºC and 5% $CO_2$. The K1-4 cell line was also cultured in DMEM+H/B Full media for maintenance of target nucleic acids.

Cell subculture was performed upon reaching ≈70% cell confluence, at that point the media is removed by aspiration with a pipette, cells are washed smoothly with PBS followed by 0.25% Trypsin-0.5µM EDTA, both at room temperature, added to the flask until cell

detachment at 37C; after cells have detached, Full media was added to inhibit Trypsin and pipetted up-and-down to detach remaining cells from the flask. Sub cultivation by transferring suspended cells to T75 flask was performed usually at 1:7 for cell maintenance and 1:4 for cell-growth for experiments.

## 2.4. Cell Plating

Cell counting and plating followed the same methodology used in cell maintenance until cell detachment by Trypsin and resuspension in Full media.
Before each experiment cells were counted to establish a standard cell number; cell counting was performed in a hemacytometer by adding a drop of suspended cells, and cells were seeded in 12-wells and 96-wells plate at $3\times10^4$ cells/well and $5\times10^3$ cells/well respectively. Cells were starved with Starved media (Serum-free) overnight prior to stimulation/treatment.

## 2.5. Cell transfection

Cells were transfected using ViaFect™ Transfection Reagent for enhanced expression of KSR1 (pcDNA3-mKSR1) and for positive control of transfection efficiency (pc-DNA-EGFP). Transfection complexes was conducted by mixing 83.3µl Serum-free OptiMEM media + 2.4µl ViaFect™ Transfection Reagent + 0,8µg DNA, incubation of the transfection complexes for 20 minutes and adding the solution to the wells of a 12-well plate with cells. The plate was placed in the incubator at 37ºC, 95% air + 5% $CO_2$. Cell transfection was performed 2 days before cell lysis for increased expression.

## 2.6. Cell Treatment and Stimulation

In this study cells were treated/stimulated with substances that required previous preparation as stated in Table 2.

*Table 2. Solutions prepared for cell treatment and stimulation*

| Solution | Composition |
|---|---|
| **1M $ZnSO_4$ (Zinc)** | 10ml – 2.87g Zinc sulfate heptahydrate - Thermo Scientific Chemicals #033399.A4 + PBS |
| **0.1µg/ml EGF** | PBS + 0.5mg/ml EGF 1:5 |
| **100mM Mercaptopyridine (Zinc Ionophore)** | 10ml – 149.15mg 2-Mercaptopyridine N-oxide sodium salt Sigma-Aldrich #H3261 + PBS |

Note: EGF was diluted from 0.5mg/ml to 0.1mg/ml in PBS immediately prior to use, further dilution to 0.1µg/ml was calculated based on the volume of media in the well at the time of stimulation.

## 2.7. Cell Treatment with $ZnSO_4$ and Epidermal Growth Factor Stimulation

$ZnSO_4$ treatment assays were performed in DU-145, PC-3 and K1-4 cell lines, cells were treated with $ZnSO_4$ with selected concentrations for 3 hours and incubated at 37ºC, 95% air + 5% $CO_2$ during the period of treatment.
In the experiments with a designated EGF exposed sample, cells were stimulated with 100ng/ml EGF in PBS for 30 minutes in the incubator at 37ºC, 95% air + 5% $CO_2$.
All experiments were performed after overnight incubation in Starved media unless otherwise specified.

## 2.8. Ionophore treatment

After overnight incubation in Starved media, DU-145 cells were treated with the Zinc Ionophore Mercaptopyridine diluted in PBS for zinc permeability at the concentrations and duration indicated in the individual experiments and incubated during the period of exposure in the incubator at 37ºC, 95% air + 5% $CO_2$.

## 2.9. Tetracycline induction

K1-4 cells were induced with 1mg/ml Tetracycline in PBS for 1 day prior to experiments to activate the tetracycline-induced target gene for enhanced KSR1 expression, cells were incubated at 37ºC, 95% air + 5% $CO_2$.

## 2.10. Western blot

Western blot technique was performed at room temperature in a clean bench, the solutions used in this technique are described in Table 3.

*Table 3. Solutions used in Western Blot*

| Solution | Composition |
|---|---|
| **Tris/Glycine/SDS Running Buffer** | 1L – 100ml 10X Tris/Glycine/SDS (0.25M Tris, 1.92M Glycine, 1% SDS) + 900ml $dH_2O$ |
| **Tris/Glycine Transfer Buffer** | 1L – 100ml 10X Tris/Glycine (0.25M Tris, 1.92M Glycine) + 900ml $dH_2O$ |
| **Tris Buffered Saline (TBS)** | 1L – 50ml 20X TBS + 950ml $dH_2O$ |
| **TBST** | 1L – 50ml 20X TBS + 950ml $dH_2O$ + 1ml Tween® 20 |
| **Blocking Buffer** | 3%BSA in TBS |
| **Primary Antibody Solution** | 5% Bovine Serum Albumin (BSA) in TBST + Antibody |
| **Secondary Antibody Solution** | 5% BSA in TBST + Antibody |
| **Triton X-100 Lysis Buffer + Protease Inhibitor Cocktail Set I** | Triton X-100 Lysis Buffer + 1X Protease Inhibitor (1:100) |

| |
|---|
| **- Calbiochem 1X (TLB + PI) (80µl/Sample)** |

## 2.10.1. Cell lysis

For cell lysis the plates were placed on ice and cells were washed 3x with ice-cold PBS and incubated for 20 minutes in 80µl of TLB + 0,8µl of PI per sample (12-wells) and 50µl of TLB + 0,5µl of PI per sample (96-wells), cells were scraped gently to detach using a cell scraper. The obtained lysate was centrifuged at 4ºC for 5 minutes at 16110 x g to separate the cell debris and the supernatant containing the proteins was saved for immunoblot analysis.

## 2.10.2. Sample preparation

Samples (55µl Sample unless otherwise specified) were prepared for immunoblot analysis by adding 4X Sample Buffer (diluted to 1X) and 1M DTT (diluted to 50mM) to the lysates as detailed in Table 4 and heated to 94ºC for 4 minutes.

*Table 4. Cell lysate preparation composition*

| Composition | 44µl Sample | 55µl Sample |
|---|---|---|
| **Cell lysate** | 31.5µl | 38.5µl |
| **4X Sample Buffer (Invitrogen NuPAGE® LDS Sample Buffer or Invitrogen Fluorescent Compatible Sample Buffer)** | 11.25µl | 13.75µl |
| **1M Dithiothreitol (DTT)** | 2.25µl | 2.75µl |

## 2.10.3. Immunoblot analysis

*Table 5. Western blot gels composition by percentage*

| Solution | 10ml Resolving Gel | | 5ml Stacking Gel |
|---|---|---|---|
| | **7.5%** | **10%** | **4%** |
| **$H_2O$** | 4.8ml | 4ml | 2.95ml |
| **30% Acrylamide/ 0.8% Bis-Acrylamide** | 2.5ml | 3.3ml | 0.7ml |
| **1.5M Tris/HCl pH 8.8** | 2.5ml | 2.5ml | N/A |
| **1M Tris/HCl pH 6.8** | N/A | N/A | 1.25ml |
| **10% SDS** | 100µl | 100µl | 50µl |
| **10% APS** | 90µl | 90µl | 45µl |
| **TEMED** | 10µl | 10µl | 5µl |

For the immunoblot analysis, Tris-Glycine (Tris-Gly) Resolving gels were prepared following the volumes described in Table 5, 10% APS and TEMED were added last and immediately before pouring the solution in the cast-cassette to initiate polymerization. SDS 0.1% was poured carefully overlaying the resolving gel in the cassette to allow a smooth surface of the resolving gel, after complete polymerization of the Resolving gel 10% APS and TEMED were added to the Stacking gel solution and immediately poured into the cassette above the Resolving gel after the removal of the 0.1% SDS, the comb was placed on the cassette before Stacking gel polymerization (30 minutes for each gel polymerization). The cassette was placed in the blot module and filled with Tris/Glycine/SDS Running Buffer, cell lysates were loaded to the cassette wells.
Western blot was performed using Invitrogen XCell SureLock™ Mini-Cell Electrophoresis Blot Module powered by Invitrogen PowerEase® 500 Power Supply.
Cell lysates were resolved by Sodium Dodecyl Sulphate-Polyacrylamide Gel Electrophoresis (SDS-PAGE) in Tris-Gly gels for 2-2,5h for 7,5% gels and 2,5h for 10% gels, both at 125V. 7,5% and 10% gels were used for KSR1 and ERK1/2 experiments respectively.
The proteins were transferred to nitrocellulose membranes at 25V for 2h and then blocked in a rocker for 1 hour in TBS+3% BSA to prevent non-specific binding of the antibodies and followed by overnight incubation at 4ºC with the primary antibodies diluted in TBST+5%BSA against the target proteins.
The membranes were washed three times (3x10minutes) with TBST after the removal of primary antibody solution and incubated with fluorescent-dye conjugated secondary antibodies diluted in TBST+5%BSA, for 1 hour in a rocker at room temperature in the dark. The secondary antibody solution was removed, and the membranes were washed again three times (3x10minutes) with TBST and ready for imaging.

### 2.10.4. Antibodies

The primary and secondary antibodies used in this study are described in Table 6 and Table 7 respectively.

**Primary antibodies**

*Table 6. Primary antibodies*

| Target | Host species | Type | Catalogue Number | Company | Dilution |
|---|---|---|---|---|---|
| **KSR1** | Rabbit | Polyclonal | #4640 | Cell Signalling Technology | 1:1000<br>1:500 |
| **KSR1** | Rabbit | Polyclonal | #PA5-75208 | Thermo Fischer | 1:500 |
| **Glu-Glu tag** | Rabbit | Polyclonal | #ab18585 | Abcam | 1:1000 |

| | | | | | |
|---|---|---|---|---|---|
| **p44/42 MAPK (ERK 1/2)** | Rabbit | Polyclonal | #91025 | Cell Signalling Technology | 1:1000 |
| **Phospho-p44/42 MAPK (p-ERK 1/2)** | Mouse | Monoclonal | #91065 | Cell Signalling Technology | 1:2000 |

**Secondary antibodies**

*Table 7. Secondary antibodies*

| Target | Host species | Colour | Catalogue Number | Company | Dilution |
|---|---|---|---|---|---|
| **Rabbit** | Goat | 800W | #926-32211 | Li-Cor | 1:20000 |
| **Rabbit** | Goat | 680RD | #926-68071 | Li-Cor | 1:5000<br>1:20000 |
| **Mouse** | Goat | 800W | #926-32210 | Li-Cor | 1:5000<br>1:20000 |
| **Mouse** | Goat | 680RD | #926-68070 | Li-Cor | 1:20000 |

### 2.10.5. Imaging Analysis

The protein bands in the membranes were analysed in a Li-Cor Odyssey® DLx Imaging System for fluorescent-dyed proteins at 680nm and 800nm for relative target protein quantification. Image Studio™ Lite Quantification Software was used for densitometry analysis.

The results were presented as the following data:

Signal (dpi): Raw numbers obtained from densitometry analysis of the bands.

% phosphorylated KSR1: The percentage of p-KSR1 was calculated using the densitometry data obtained in the equation $\%p\text{-}KSR1 = \frac{pKSR1}{pKSR1+KSR1} \times 100$ .

Fold change: For KSR1 protein, Fold change was calculated by normalizing the densitometry data to the Control cells. For p-ERK 1/2 protein, the ratio of p-ERK1/2 /t-ERK 1/2 per sample was calculated from densitometry data and then normalized to the Control cells.

Densitometry data was analysed in Microsoft Excel and GraphPad Prism, graphs were drawn in GraphPad Prism.

### 2.10.6. Statistical Analysis

The statistical analysis of eligible experiments for the significance of phosphorylation differences was performed using One-Way ANOVA followed by Tukey's HSD test ($\alpha$=0.05) in GraphPad Prism.

## 2.11. MEK1/2 and KSR1 Inhibitors Assay

K1-4 cells were treated with PD184352 (CI-1040) MEK1/2 Inhibitor (APEXBIO) and APS-2-79 KSR Inhibitor (MedChemExpress) to study ERK 1/2 activity cell growth assessment. Cells were plated in 96-Wells plate (12 wells per inhibitor) with 0.2ml DMEM+H/B Full media at a concentration of $5\times10^3$ cells/well and incubated at 37ºC, 95% air + 5% $CO_2$ overnight prior to the start date of the experiment. The inhibitors were diluted in DMSO (1:200 dilution) at the selected and added to the wells; EGF+DMSO cells were treated with 100ng/ml EGF + DMSO (1:5 dilution).
To study the importance of ERK and KSR1 in cell growth under the influence of PD184352 MEK and APS-2-79 KSR inhibitors (concentrations in a range of 1µM, 5µM and 10µM) the plates were placed in the MuviCyte™ live-cell imaging kit (incubated at 37ºC and5% $CO_2$) for 65 hours time-course and cell confluence was measured every 5 hours.

*Table 8. Concentration of stock inhibitors*

| Inhibitor | Concentration |
|---|---|
| **5mg PD184352 (CI-1040) MEK** | 10mM PD184352 (CI-1040) in DMSO |
| **5mg APS-2-79 KSR** | 10mM APS-2-79 KSR in DMSO |

### 2.11.1. Imaging analysis

Cell confluence data obtained from the The MuviCyte™ live-cell imaging kit (PerkinElmer) was analysed using GraphPad Prism; following logarithmic transformation of the confluence values, linear regression was applied, and the obtained slope of the line was used for graph drawing and interpretation.
Graphs representing the percentage of confluence were drawn from the confluence values for a visual representation.

## 2.12. E. coli transformation and plasmid isolation

One Shot™ TOP10 Chemically Competent E. coli (Thermo Fisher) were used for transformation with pcDNA3-mKSR1.
For this technique, 1µl of stock plasmid was added to the One Shot™ TOP10 Chemically Competent E. coli vial and incubated on ice for 30 minutes. After that, it was treated with heat shock by 30 seconds incubation in a 42ºC water bath and placed again on ice.
250µl of LB media was added to the vial and incubated in a shaking incubator at 37ºC and 225 rpm for 1 hour, then 100µl was removed from the vial and plated in a p100 Petri dish with LB agar + 0.1mg/ml Ampicillin followed by overnight incubation at 37ºC (inverted position to prevent water condensation).
Isolated colonies were selected for each assay, inoculated in 5ml of LB media + 0.1mg/ml Ampicillin, incubated overnight at 37ºC and 175 rpm in a rotary shaker following a second

inoculation by adding one drop from the 5ml cell/media solution to 100ml of LB media + 0.1mg/ml Ampicillin and incubated overnight at 37ºC and 175 rpm.
PureYield™ Plasmid Midiprep System was used for cell lysis and plasmid extraction and purification:
The cells were centrifuged for 10 minutes at 5000 x g, and the pellets were resuspended in Cell Resuspension Solution (50mM Tris-HCl pH 7,5 + 10mM EDTA pH 8 + 100µg/ml RNase A) and lysed with Cell Lysis Solution (0,2M NaOH + 1% SDS).
Cell lysis was stopped with Neutralization Solution (4.09M Guanidine Hydrochloride pH 4,2 + 759mM Potassium Acetate + 2.12M Glacial Acetic Acid) and cells were centrifuged at 5000 x g for 20 minutes.
Lysates were washed with Endotoxin Removal Wash and Column Wash Solution (162,8mM Potassium Acetate + 22,6mM Tris-HCl pH 7,5 + 0,109mM EDTA pH 8.0) in the column stack with vacuum system.
Plasmid was eluted using the Eluator™ Vacuum Elution device, the Plasmids purified by ethanol precipitation with 99% ethanol and washed with 70% ethanol. Plasmids were then analysed in a NanoDrop system to determine DNA concentration and quality before storing at -20ºC.

# 3. Results

## 3.1. Analysis of zinc exposure on KSR1 and ERK1/2 phosphorylation in DU-145 cells

To investigate the effect of zinc on KSR1 phosphorylation, we performed analysis on cell lines Du-145 and PC-3 to determine the expression and phosphorylation levels of KSR1 (Wt and mutants). Additionally, we assessed the expression and phosphorylation of ERK 1/2 under different experimental conditions.

### 3.1.1. Characterisation of KSR1 expression in prostate cancer cell lines

Preliminary results obtained in our laboratory suggested different expression levels of KSR1 between prostate cancer cell lines. As such we found it relevant to perform a screening on the KSR1 expression levels in DU-145, PC-3 and LNCaP cells to evaluate which cell line(s) would be most suitable for the planned studies.
To analyse the presence of KSR1 in the three Prostate cancer cell lines, cell lysates from each cell line were resolved by SDS-PAGE in a 7,5% gel and analysed by Western Blot with two different concentrations of α-KSR1 primary antibody.

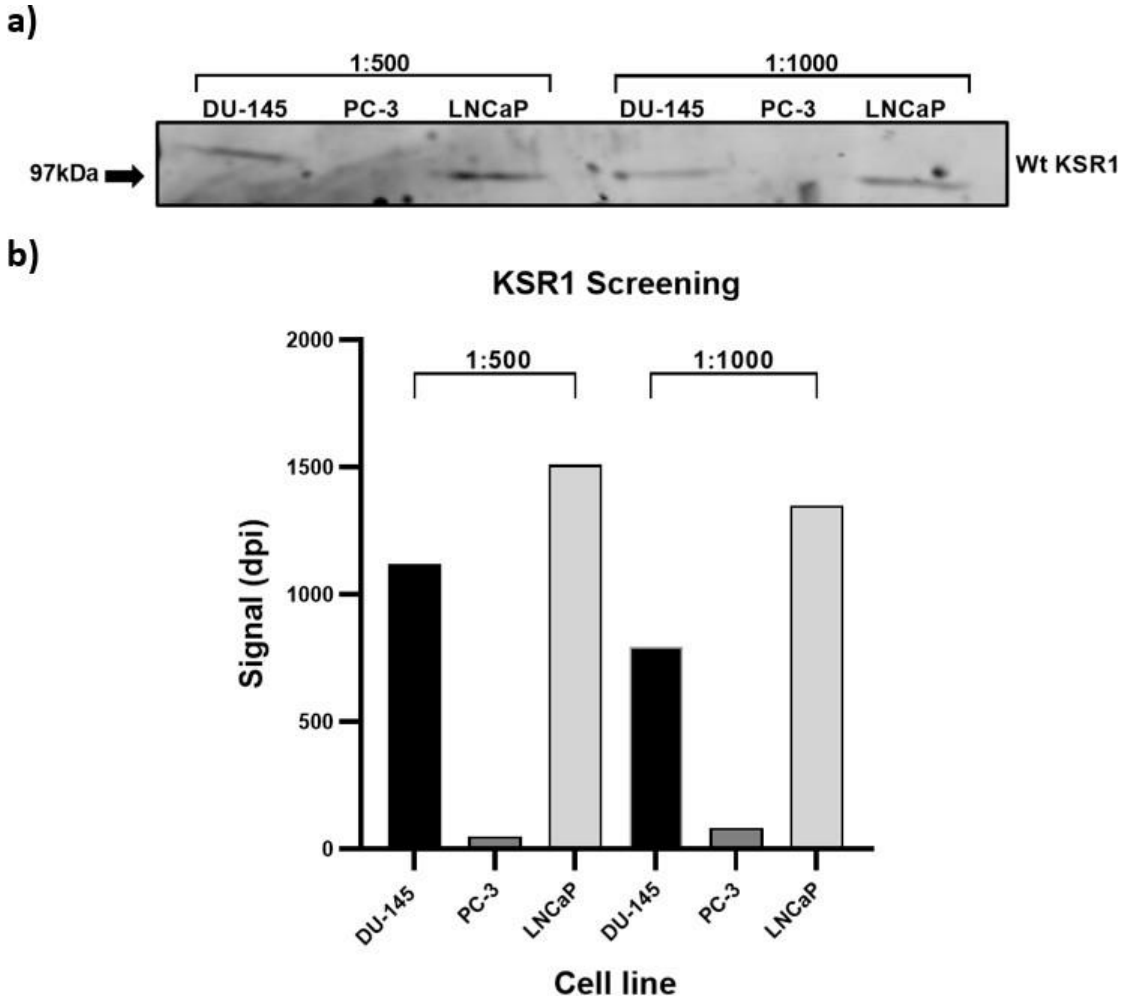


*Figure 5. Western blot analysis of KSR1 expression in DU-145, PC-3 and LNCaP cell lines. a) Western blot showing KSR1 expression in DU-145, PC-3 and LNCaP cell lines as detected with α-KSR1 antibody (CST #4640) at two different dilutions (1:500 and 1:1000 concentrations).; b) Quantification of KSR1 expression by densitometry of the blot shown in a). Raw data are shown without normalisation. N=1*

Results showed (Figure 5) an enhanced detection of KSR1 expression with the highest concentration (1:500) of α-KSR1 4640 CST primary antibody, confirming previous results from the research group, as well as a barely detectable signal of KSR1 in PC-3 cells when compared to the DU-145 and LNCaP cell lines. This suggests that PC-3 cells have a reduced expression of KSR1 that may not be detectable in western blot analysis. However, DU-145 and LNCaP present clear bands of KSR1 in Figure 5.a at the correct molecular weight (97kDa).

This indicated the DU-145 as the preferable cell line for primary experiments regarding KSR1 expression and phosphorylation, based on the detectable expression of KSR1 and the easier handling of the cells.

### 3.1.2. Evaluation of DU-145 transfection efficacy and characterization of pcDNA3-mKSR1 plasmid

As seen in the previous section, the prostate cancer cell lines express detectable but not very strong KSR1 levels, transfection with a KSR1 plasmid was necessary to increase KSR1 expression and therefore ensure the results.

The optimization of the transfection technique was performed on the DU-145 cell line by transfecting the cells with pcDNA-EGFP plasmid as a control using different transfection reagents - Viafect™ Transfection Reagent, Lipofectamine™ and Fugene® 6 – to determine the most effective reagent (data not shown). The optimal period of transfection was also assessed (2 days vs. 1 day). The result of this experiment indicated the Viafect™ Transfection Reagent as the optimal transfection technique and 2 days as the optimal transfection period.

Considering that the DU-145 cell line is known to be difficult to transfect, the K1-4 cell line was used as a positive control of transfection since it is transfected easily.

We then seeded the cell lines in 12-Wells plate until 70% confluence, transfected DU-145 and K1-4 cells using Viafect™ Transfection Reagent (as described in section 2.2.4) with pcDNA-EGFP (GFP) to compare transfection efficacy and incubated 2 days for enhanced expression.

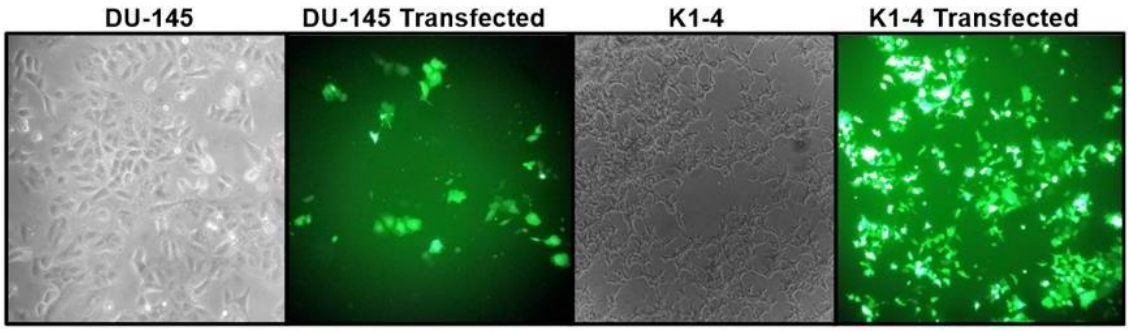


*Figure 6. Transfection of DU-145 and K1-4 cell lines with GFP plasmid for transfection efficacy. Cells transfected with GFP using Viafect Transfection Reagent and 2 days of incubation before transfection assessment; images captured with and without UV light. N=1*

Figure 6 shows the transfection of DU-145 which is lower than the K1-4 cells but sufficient for detection in Western blot analysis.
Next, we tested whether transfection of KSR1 would increase the signal in western blotting analyses. Cells were seeded in 12-wells plate and grown until 70% confluency. Cells were then transfected with pcDNA3-EGFP and pcDNA3-mKSR1 plasmids (Figure 7) 2 days prior

to the Western Blot analysis. Cell lysates were resolved by SDS-PAGE in a 7,5% gel and analysed by Western Blot. Image Studio Lite was used for densitometry analysis.

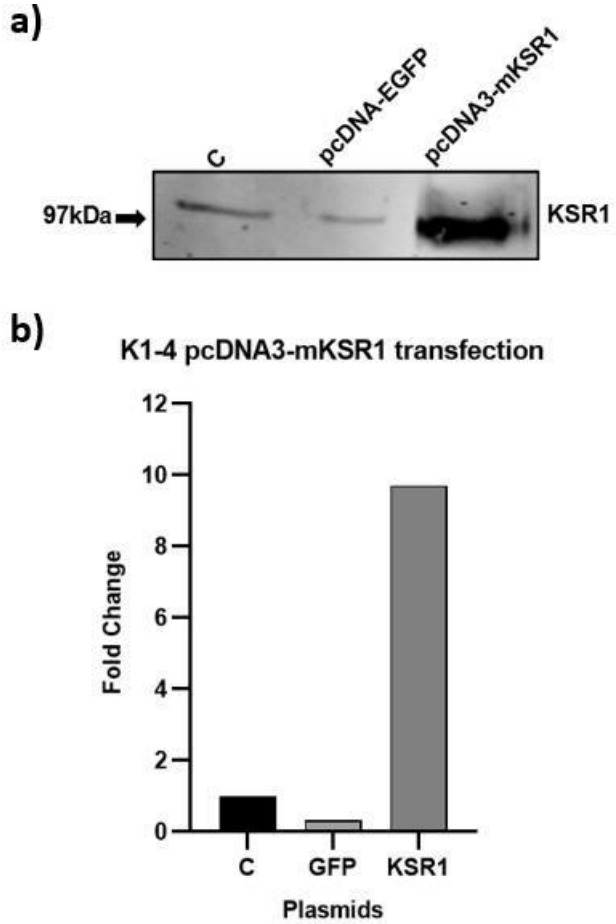


*Figure 7. Transfection of K1-4 cells with pcDNA-EGFP (GFP) and pcDNA3-mKSR1 (KSR1) for protein expression and transfection efficacy assessment via Western Blot analysis (detected using α-KSR1 PA5-75208 antibody in 1:500 concentration) (a) and fold change variation (b). Data obtained from densitometry and normalized to Control; N=1*

The results demonstrate successful transfection of pcDNA3-mKSR1 since the band corresponding to KSR1 is strongly detected in Figure 7.a and has an increased expression level of almost 10 times compared to the control (Figure 7.b). This confirms the effectiveness of the Viafect Transfection Reagent technique in this cell line and plasmid efficiency in overexpressing KSR1, thus validating pcDNA3-mKSR1 transfected DU-145 experiments.

## 3.2. Effect of zinc treatment on the phosphorylation of KSR1 in DU-145 cells

In order to investigate the effect of zinc exposure on KSR1 phosphorylation in DU-145 cells we treated Wt and Transfected DU-145 cells with different concentrations of $ZnSO_4$. Cells were seeded in 12-well plates and allowed to grow overnight (70% confluency). DU-145 cells were either left untransfected or were transfected with pcDNA3-mKSR1 2 days prior

to Western Blot analysis. Cells were serum starved in the following day and incubated for 16 hours and then treated with $ZnSO_4$ for 3 hours at concentrations of 50µM, 200µM, 500µM and 1000µM, and EGF for 30 minutes as depicted in Figure 8.a. Cells were lysed in TLB+PI and lysates were resolved by SDS-PAGE in 7,5% Gel and analysed by Western Blot.

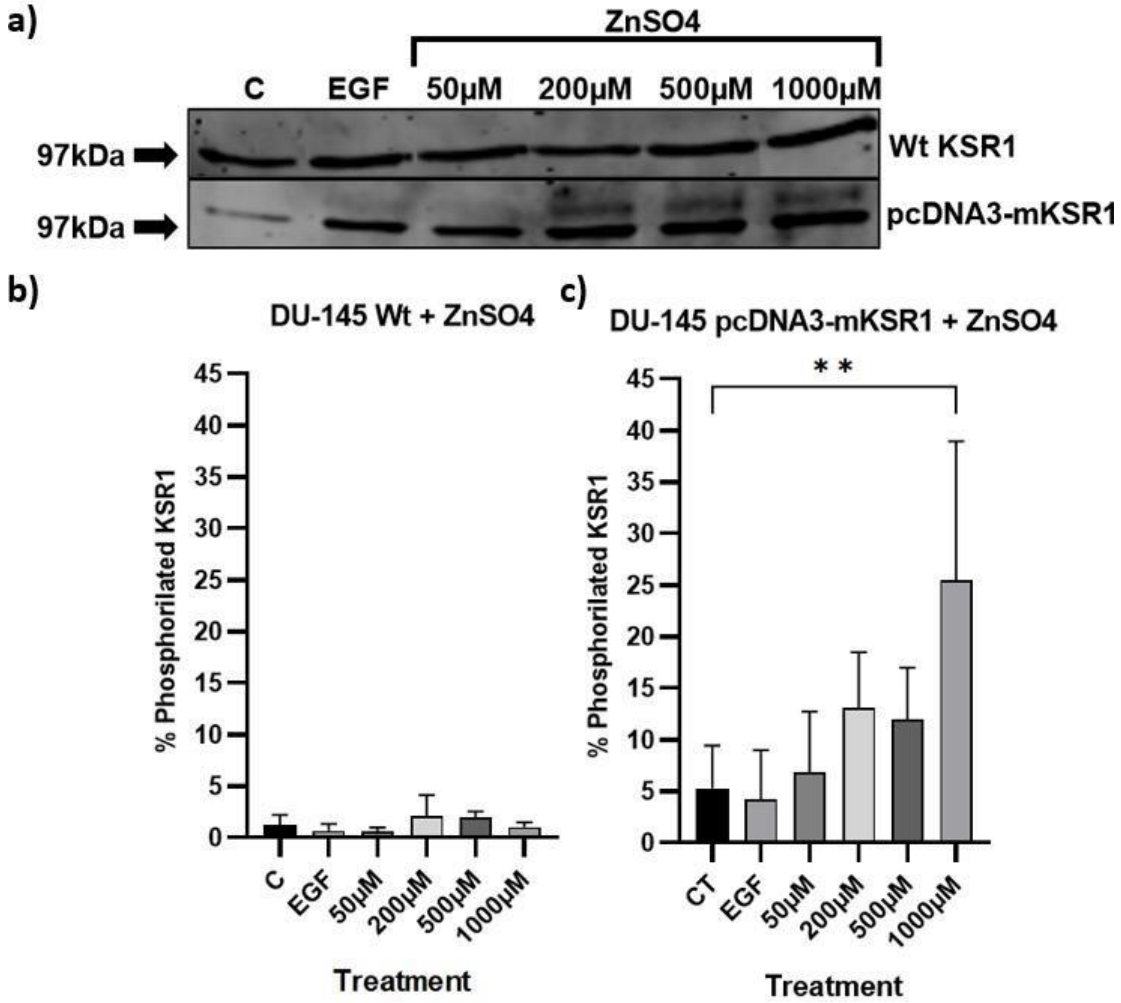


*Figure 8. Western Blot analysis of the effect of EGF and $ZnSO_4$ treatment in DU-145 cells (Wt and Transfected) KSR1 phosphorylation in the range of concentration of 50µM to 1000µM; a) Wt KSR1 and pcDNA3-mKSR1 expression and phosphorylation after $ZnSO_4$ and EGF treatment; b) percentage of phosphorylation of Wt KSR1 after $ZnSO_4$ and EGF treatment. c) percentage of phosphorylation of pcDNA3-mKSR1 after $ZnSO_4$ and EGF treatment. Means + Standard deviation. Percentage of phosphorylation calculated from densitometry data (Section 2.3.5). KSR1 and p-KSR1 was detected using α-KSR1 PA5-75208 antibody in a 1:500 concentration. N=3*

The results showed that a $ZnSO_4$ induced mobility shift of KSR1, indicating KSR1 phosphorylation, can only be seen in transfected cells (Figure 8.a). Figure 8.c depicts the increased KSR1 phosphorylation by increasing Zinc concentration, with the highest level of zinc corresponding to the highest percentage of phosphorylation compared to the control -

1000µM of $ZnSO_4$ resulted in 25% of KSR1 phosphorylation (p-value: 0.0095; confidence level: 95%).

### 3.2.1. Assessment of KSR1 phosphorylation increase with elevated Zinc concentrations

As it is seen in Figure 8.a, KSR1 phosphorylation by zinc induction in DU-145 cell line was not complete as it was shown in HEK 293 cells previously [46]. Due to this, we decided to test higher concentrations of zinc (50µM to 4000µM for DU-145 Wt; 500µM to 4000µM for DU-145 Transfected) (Figures 9.a and 9.c). As in the previous experiment, cells were seeded in 12-Wells plate and, after overnight incubation, half of the samples were transfected with pcDNA3-mKSR1. In the following day Wt and Transfected cells were serum starved for 16h and then treated with $ZnSO_4$ for 3 hours with the concentrations described above, and with EGF for 30 minutes. Lysates were resolved by SDS-PAGE in 7,5% gel and analysed by Western Blot.

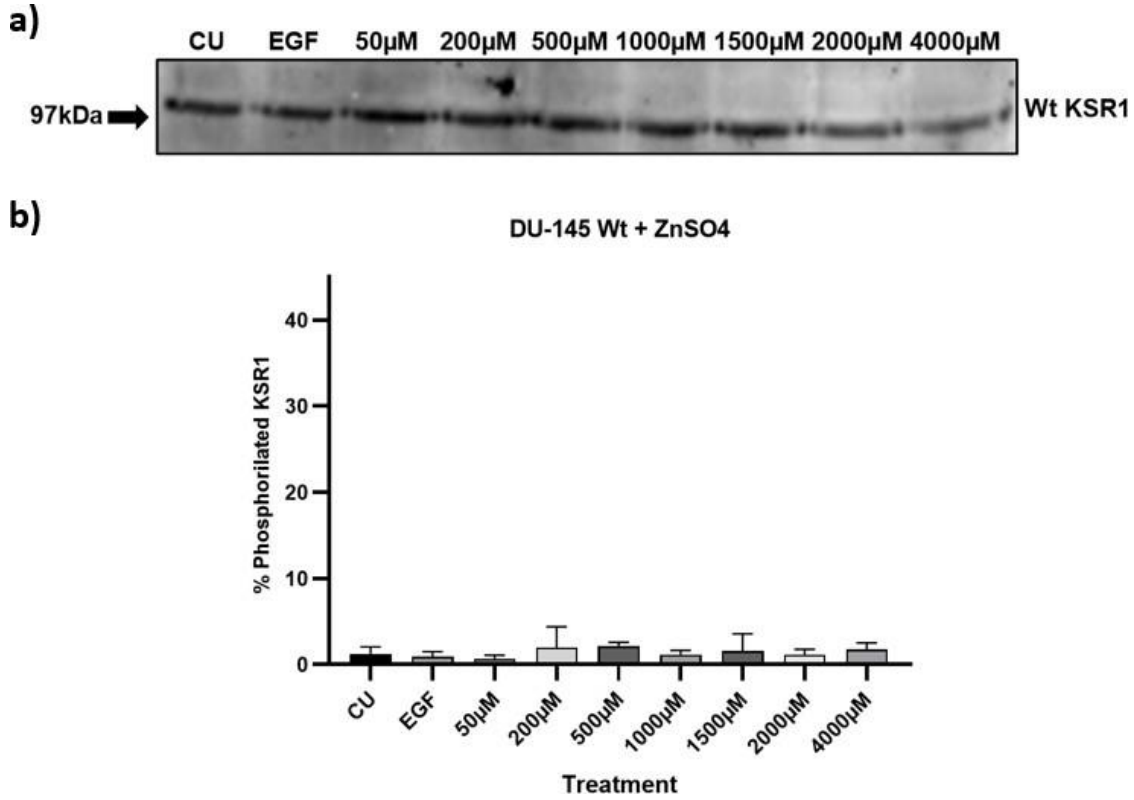

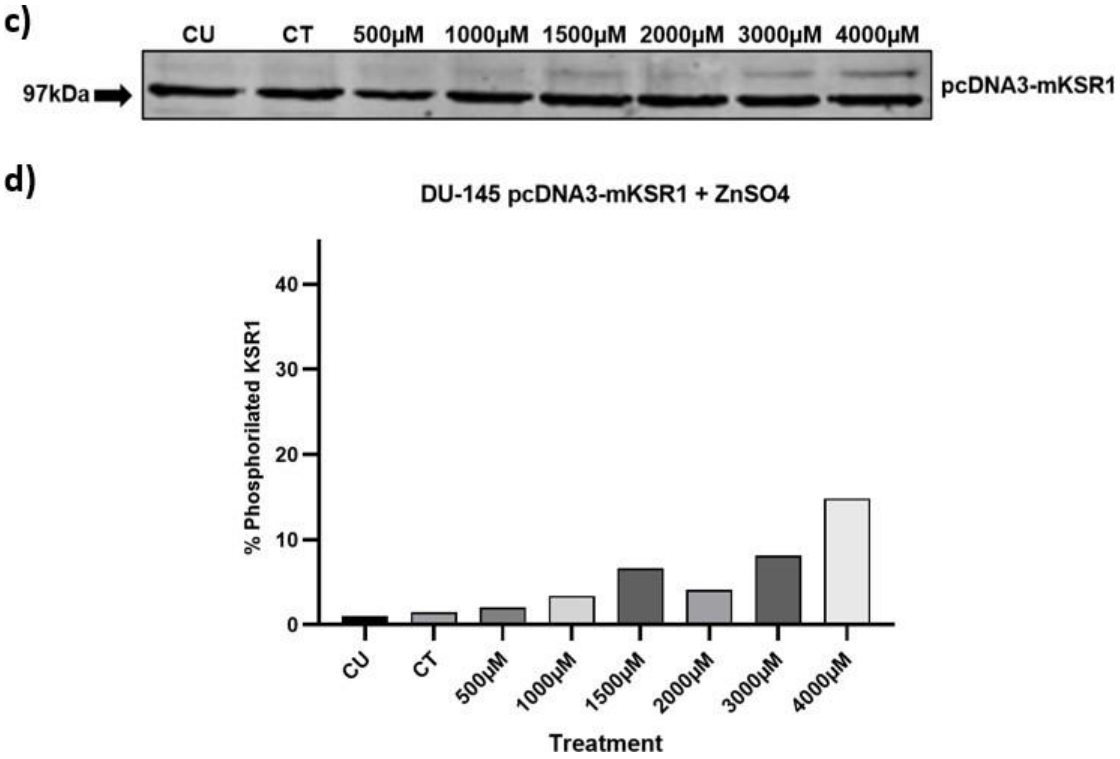


*Figure 9. Western Blot analysis of $ZnSO_4$ effect on KSR1 phosphorylation in Wt DU-145 and Transfected DU-145 in increased concentrations up to 4000µM. a) Wt KSR1 bands under $ZnSO_4$ treatment with no apparent phosphorylation. b) Densitometry analysis of Wt p-KSR1 bands under $ZnSO_4$ treatments. c) pcDNA3-mKSR1 bands under $ZnSO_4$ treatment with no apparent phosphorylation. d) Densitometry analysis of p-pcDNA3-mKSR1 bands under $ZnSO_4$ treatments. Percentage of phosphorylation calculated from individual values obtained from densitometry. KSR1 proteins (a) and (b) were detected using α-KSR1 PA5-75208 antibody in 1:500 concentrations. N=1*

The results of KSR1 phosphorylation screening indicate that the increase of $ZnSO_4$ to more than 1000µM enhances the phosphorylation of KSR1 in transfected DU-145 cells, noticeable in Figure 9.c and Figure 9.d. As shown in figure 8.b, the percentage of phosphorylation appears to increase with high concentrations of zinc (1000µM) , accordingly, the Figure 9.b ensures this correlation with higher concentrations (4000µM).
However, as depicted in Figures 8.a and 8.b, and evident from Figures 9.a and 9.b, the p-KSR1 bands are not detectable in Wt DU-145 cells when exposed to the various concentrations of $ZnSO_4$, as tested.

### 3.2.2. Treatment of DU-145 cells with Zinc Ionophore Mercaptopyridine for increased $ZnSO_4$ uptake

It is well known that advanced prostate cancer cells have lost expression of zinc transporters, which could cause a reduction in their ability to uptake zinc. This correlates with our observation that KSR1 phosphorylation is only partially induced by $ZnSO_4$ treatment in DU-145 cells. To test whether an increase in zinc transport would increase KSR1 phosphorylation, two experiments were conducted with Zinc and Zinc Ionophore Mercaptopyridine combination treatment to access phosphorylation and toxicity.
Cells for both experiments were seeded in 12-well plates and incubated overnight. Cells were starved with serum starved media for 16 hours and, in each experiment, cells were treated with $ZnSO_4$ and the zinc ionophore Mercaptopyridine as described below. Cells were lysed with TLB+PI and the lysates were resolved by SDS-PAGE in a 7,5% Gel and analysed by Western Blot. Primary antibody α-KSR1 PA5-75208 was used in a 1:500 concentration to detect KSR1.

Firstly, we tested a constant concentration of Zinc Ionophore (5µM) and different concentrations of zinc (0,1µM, 0,5µM, 1µM, 5µM,10µM and 20µM) (Figure 10.a). Differently to the experiment in Figure 9, we decided to lower the concentrations of Zinc compared to the previous experiment due to the presence of Zinc Ionophore since it increases membrane permeability to zinc, the concentrations previously used could be toxic to the permeabilized cells.

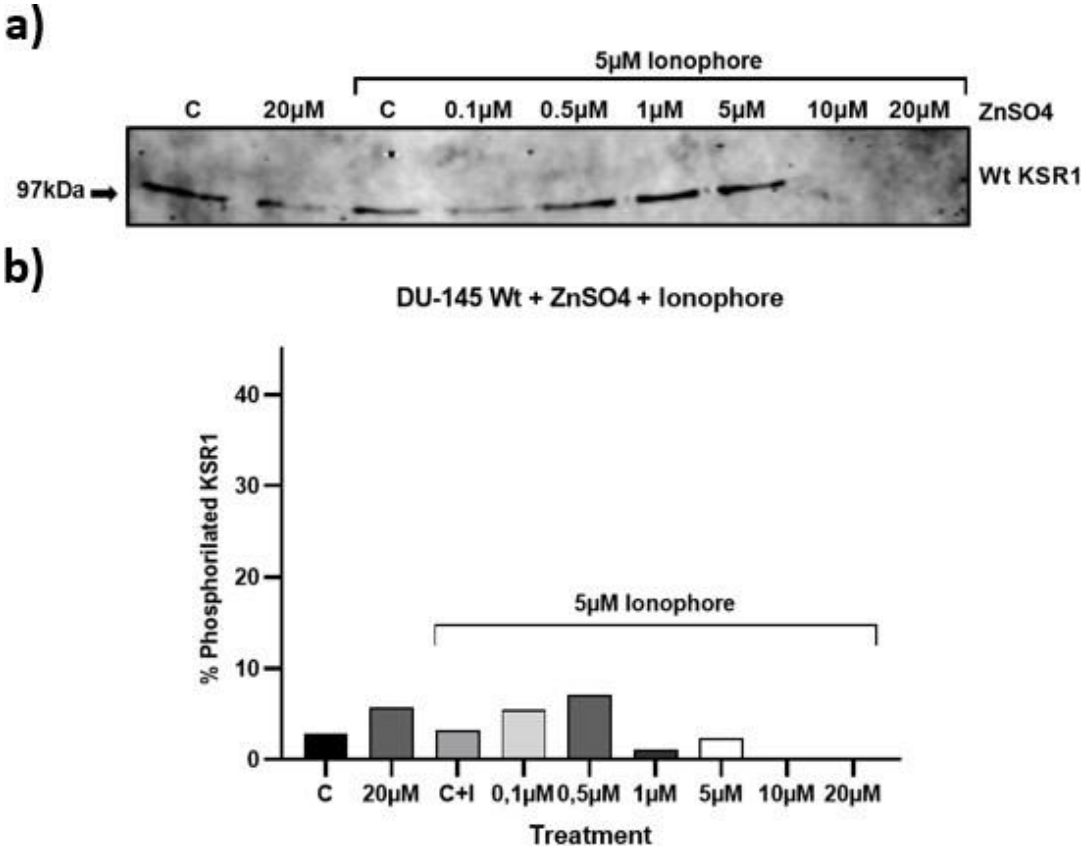


*Figure 10. a) Western Blot results of increasing concentrations of $ZnSO_4$ (0,1μM, 0,5μM, 1μM, 5μM,10μM and 20μM) and constant concentration of Ionophore (5μM) combination effect on KSR1 phosphorylation b) Densitometry analysis of the percentage of Wt KSR1 phosphorylation under increasing $ZnSO_4$ concentrations and 5μM Zinc Ionophore treatment. p-KSR1 proteins (a) and (b) were detected using α-KSR1 PA5-75208 antibody in 1:500 concentrations. N=1*

The results demonstrate that the concentrations of $ZnSO_4$ and Zinc Ionophore used are unable to induce KSR1 phosphorylation. However, Figure 10.a shows that KSR1 could not be detected when the cells were treated with 5μM Zinc Ionophore and 10 μM and 20μM of $ZnSO_4$, indicating that these combinations may be toxic to DU-145 cells.

Secondly, due to the indicative toxicity observed above with 5μM Zinc Ionophore and 10 μM and 20μM of $ZnSO_4$, we tested a constant concentration of zinc (5μM), that was not perceived as toxic in Figure 10, and different concentrations of Zinc Ionophore (5μM, 2,5μM, 1μM, 5μM, 2,5μM, 1μM, 2,5μM and 1μM) but with an increased time of treatment in a time course of 9h (9h, 6h and 3h) (Figure 11).

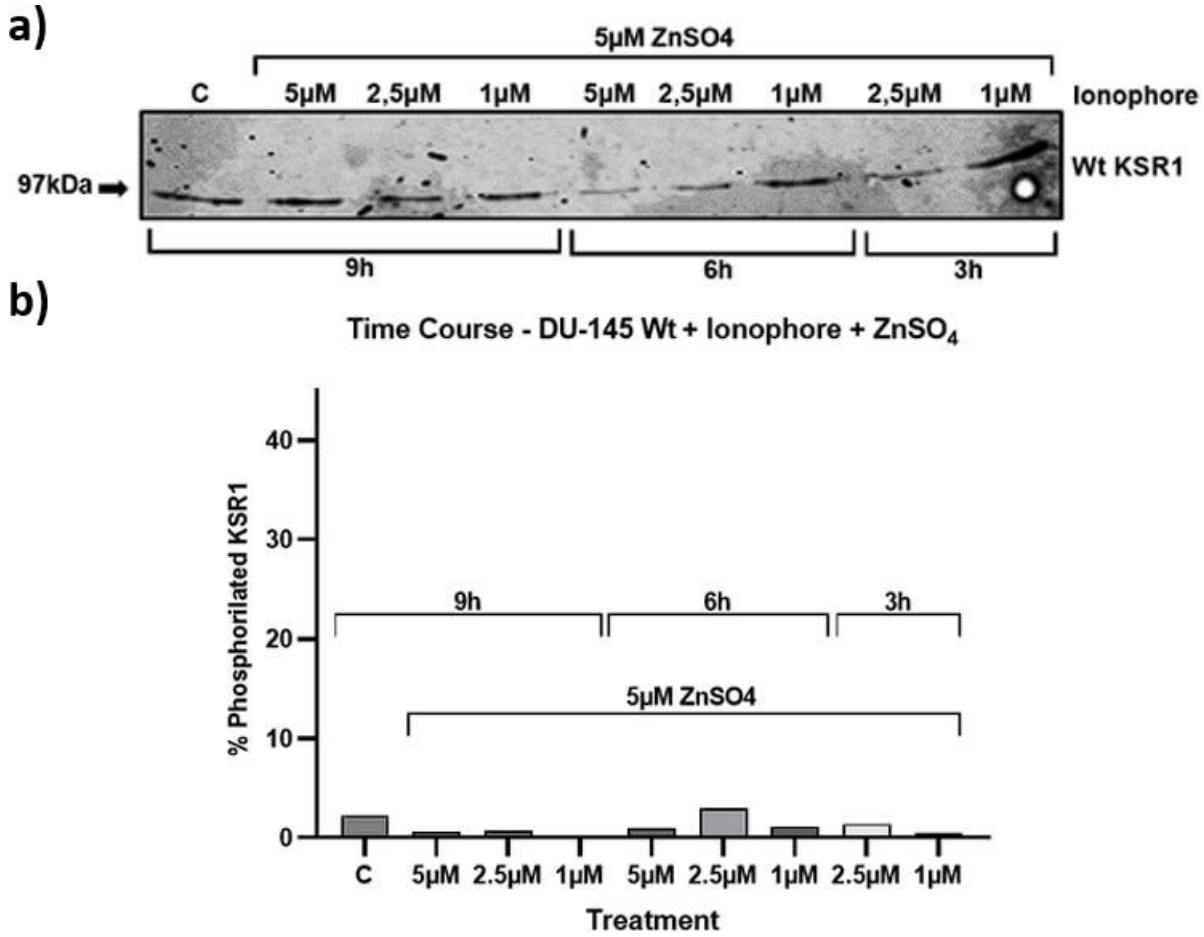


*Figure 11. c) Western blot results of the interaction of 5µM, 2,5µM and 1µM of $ZnSO_4$ and 5µM Zinc Ionophore in Wt p-KSR1 expression over a time course of 9 hours, 6 hours and 3 hours (5µM $ZnSO_4$ + 5µM Ionophore for 3 hours had already been performed in Figure 10; d) Densitometry analysis of the percentage of Wt KSR1 phosphorylation with different concentrations of $ZnSO_4$ (described in Figure 6.c) and 5µM Zinc Ionophore treatment during 9 hours, 6 hours and 3 hours. Percentage of phosphorylation calculated from densitometry data. p-KSR1 proteins (c) and (d) were detected using α-KSR1 PA5-75208 antibody in 1:500 concentrations. N=1*

The reduction of the combined concentrations of $ZnSO_4$ and Zinc Ionophore appears to solve the toxicity of these substances on the cells. However, despite the combinations of concentrations used and periods of exposure, there was no phosphorylation of KSR1 since only Wt-KSR1 bands were detected (Figure 11).

### 3.2.3. The combination of zinc and ionophore is toxic in DU-145 cells

Hereupon we proposed to access cell behaviour towards Zinc and Zinc Ionophore combination to understand which treatment is toxic to the cells based its behaviour in vitro, allowing us to define the optimal concentrations below toxic levels.
DU-145 cells were seeded in 12-Wells plate and allowed to grow overnight, cells were then treated with $ZnSO_4$ in different concentrations previously used (20µM, 50µM and 100µM) and a constant concentration of Zinc Ionophore (2,5µg/ml) for 3 hours. Cells were analysed by microscopy for morphology and cell survival.

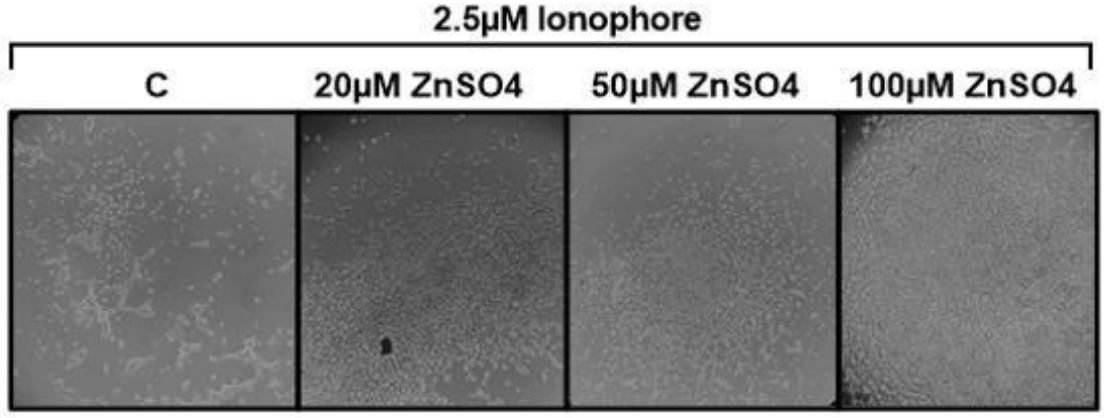


*Figure 12. Impact of Zinc and Zinc Ionophore in DU-145 cells. Control cells (C) shows live attached cells with space in-between under 2,5µM Ionophore treatment; 20µM, 50µM and 100µM $ZnSO_4$ cells shows detached round and clump-centralized forming dead cells.*

Figure 12 confirms that Zinc Ionophore singly used at lower concentrations (C) does not present toxicity since cells are attached to the well surface and randomly dispersed; but its combination with previously used $ZnSO_4$ concentrations resulted in cell detachment and death, observable in the round floating cells that merged into clump-like forms in the centre of the well.
As the concentrations of Zinc that allow cell survival in combination with Zinc Ionophore (Figure 11) did not induce KSR1 phosphorylation and higher concentrations proved toxic to the cells, Mercaptopyridine was not used any further in this study.

### 3.2.4. The effect of Zinc treatment on ERK 1/2 activity in DU-145 Transfected cells

Based on the previous results that zinc treatment induces KSR1 phosphorylation, the effect of zinc exposure of DU-145 cells on ERK 1/2 activity was studied. For that, screening for Transfected KSR1 induced ERK 1/2 phosphorylation was performed in full and starved media to understand ERK 1/2 activity when induced with EGF (KSR1+EGF) and treated with 1000µM $ZnSO_4$ (KSR1+$ZnSO_4$) in basal and stimulated levels.
Cells were seeded in 12-Wells plate and allowed to grow overnight until 70% confluence; transfection with pcDNA-EGFP was performed 2 days before Zinc treatment and was used

as a positive control of transfection and as a control cells since it does not affect KSR1 or ERK 1/2 activity.

In the following day Starved cells were incubated in serum-free media for 16 hours and then treated with 1000µM $ZnSO_4$ for 3 hours and EGF for 30 minutes. Cells were lysed in TLB+PI and the lysates were resolved by SDS-PAGE in a 10% Gel and analysed by Western Blot.

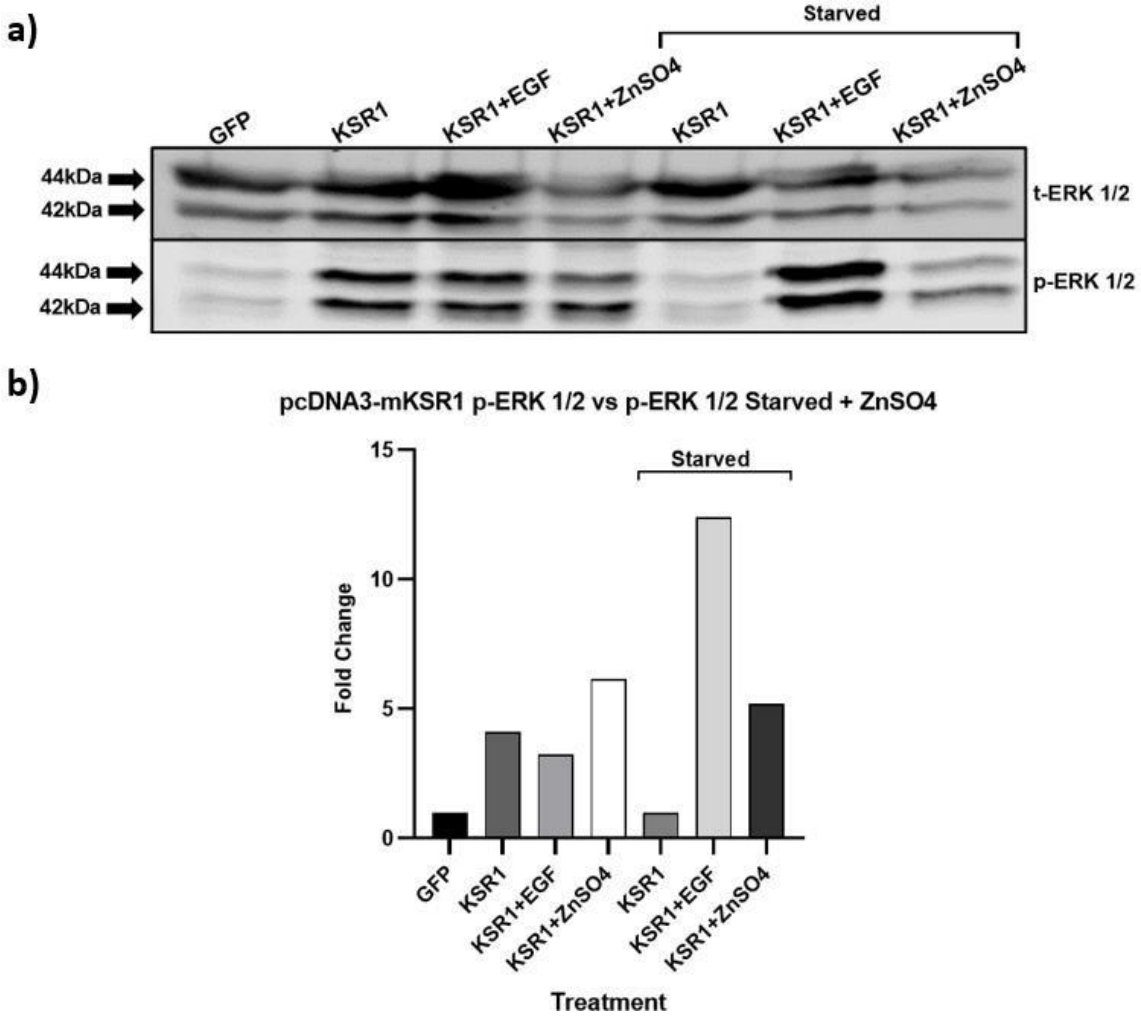


*Figure 13. Western blot analysis of EGF and $ZnSO_4$ in ERK 1/2 activity of Transfected DU-145 cells in Full and Starved media a) t-ERK 1/2 and p-ERK 1/2 bands after EGF and 1000µM $ZnSO_4$ treatment in Full and Starved media. b) Fold change in ERK 1/2 phosphorylation after EGF and 1000µM $ZnSO_4$ treatments in Transfected DU-145 cells in Full and Starved media. Data obtained by densitometry and normalised to the GFP cells. ERK 1/2 and p-ERK 1/2 proteins were detected using α-t-ERK 1/2 Rabbit 91025 and α-p-ERK 1/2 Mouse 91065 antibodies with a concentration of 1:5000. N=1*

Transfected cells (KSR1) in full media showed higher ERK 1/2 activation compared to the Control (GFP). In these cells, the ERK 1/2 phosphorylation was not affected by the addition of EGF to the media, however it was slightly increased upon $ZnSO_4$ treatment.

On the contrary, transfected cells which were serum starved presented a lower activation of ERK 1/2 compared to transfected cells in full media, while p-ERK 1/2 levels were spiked after treating the cells with EGF and with $ZnSO_4$.

The results shown were obtained from one experiment (n=1), therefore further experiments are required to ensure the accuracy of data.

### 3.2.5. Treatment of DU-145 Transfected cell line with increasing Zinc concentrations for ERK 1/2 phosphorylation evaluation

The next objective had the purpose of observing phosphorylation of ERK 1/2 induced by phosphorylated KSR1, using increasing concentrations of $ZnSO_4$ (50µM, 200µM, 500µM and 1000µM).
To analyse that, cells were seeded in 12-Wells and allowed to grow overnight until 70% confluency. DU-145 cells were transfected with pcDNA3-mKSR1 2 days prior to Western Blot analysis; cells were starved with serum-free media in the next day and incubated for 16 hours, after that $ZnSO_4$ treatment was applied to the cells for 3 hours.
EGF was used as a positive control for 30 minutes; Transfected and non-Transfected controls (CT and CU respectively) were used as shown in Figure 14.a. Non-transfected controls were used to determine if higher KSR1 expression has an effect on ERK1/2 activation in the absence of growth factor treatment. Cells were lysed with TLB+PI and lysates were resolved by SDS-PAGE in 10% Gel and analysed by Western Blot.

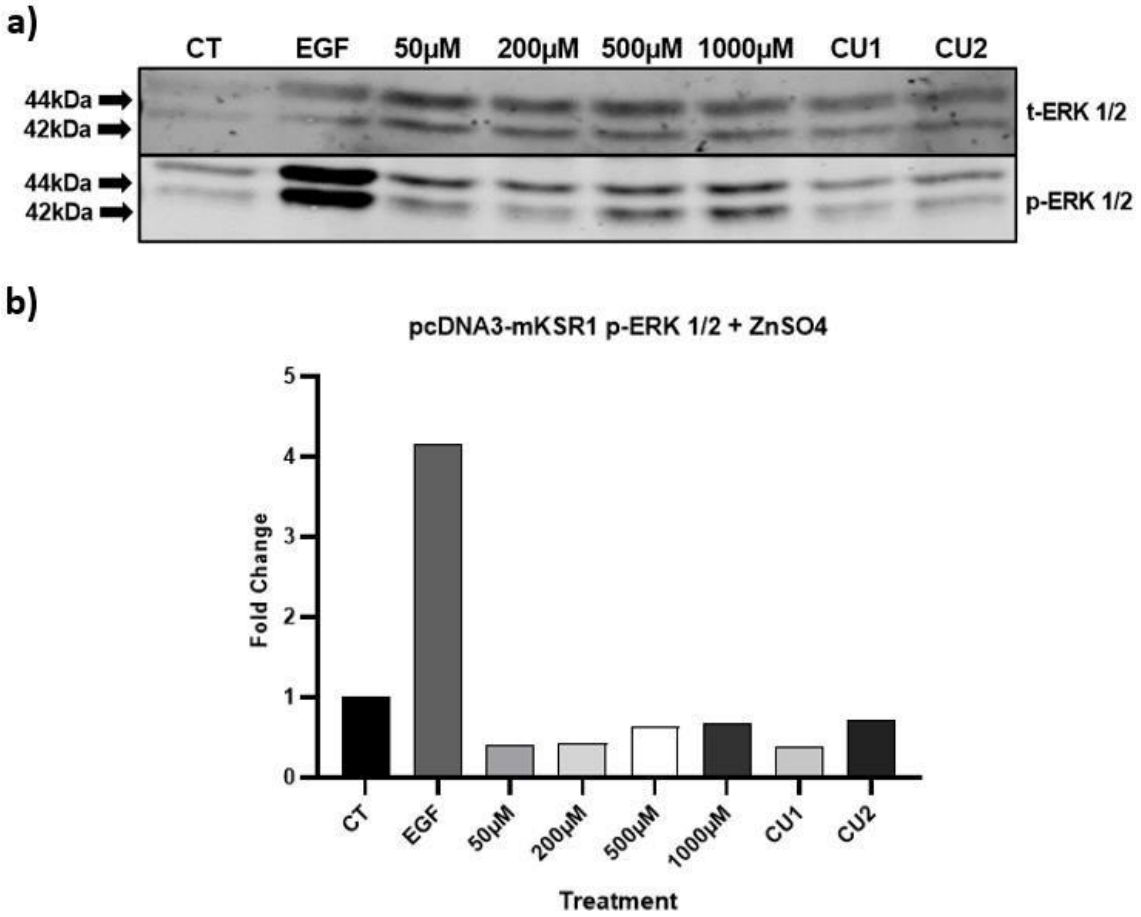


*Figure 14. Western blot analysis of the effect of different $ZnSO_4$ concentrations on ERK1/2 phosphorylation of DU-145 transfected cells; a) t-ERK 1/2 and p-ERK 1/2 bands after $ZnSO_4$ treatments; b) Fold change in ERK 1/2 phosphorylation after $ZnSO_4$ treatments in Transfected DU-145 cells. Data obtained by densitometry and normalised to the Control Transfected (CT) cells; EGF treated cells were used as a positive control and two non-transfected controls (CU1 and CU2) were used to observe differences to transfected control (CT). ERK 1/2 and p-ERK 1/2 proteins were detected using α-t-ERK 1/2 Rabbit 91025 and α-p-ERK 1/2 Mouse 91065 antibodies with a concentration of 1:5000. N=1*

The results portray a high EGF-induced phosphorylation of ERK 1/2 and a slight increase in p-ERK 1/2 expression between increasing Zinc concentrations. However, all the Zinc-induced cells exhibit lower p-ERK 1/2 levels compared to the Transfected Control (CT). Transfected Control and Non-transfected controls (CU1 and CU2) present similar bands of p-ERK 1/2 (Figure 14.a)

Contrarily to Figure 14.b results, in Figure 14.a t-ERK 1/2 is strongly expressed in Zinc treated cells (50Z to 1000Z) compared to CT, CU1 and CU2. Still, ERK 1/2 is less phosphorylated in Zinc treated cells than in CT.

### 3.2.6. Zinc treatment in the PC-3 cell line

In order to validate and extend the results obtained from the experiments conducted on the DU-145 cell line, we considered it was relevant to include another Prostate cancer cell line in this study to evaluate the generalizability and reproducibility of the observed results.
To accomplish this, we selected the PC-3 cell line that shares relevant characteristics with the DU-145 cell line used in the initial experiments. This selection ensures that the chosen cell line is representative of the biological context and allows for meaningful comparisons since it is also an androgen-independent cell line.
We utilised similar concentrations of Zinc used in the DU-145 cells (Figures 8.a and 9.a). PC-3 cells were seeded in 12-Wells plate and incubated overnight to allow cell growth, afterward the cells were starved with serum-free media for 16 hours and treated with $ZnSO_4$ for 3 hours and induced with EGF for 30 minutes as depicted in Figures 15.a and 15.b; cells were lysed with TLB+PI; the lysates were resolved by SDS-PAGE in 7,5% Gel and analysed by Western Blot.

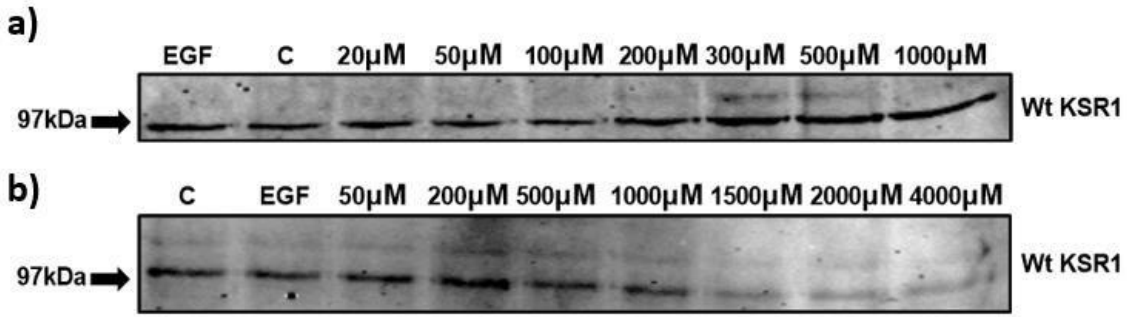


*Figure 15. Western Blot analysis of $ZnSO_4$ treatment effect on PC-3 cell line KSR1 phosphorylation. Treatment of PC-3 cell line with EGF and 20µM to 1000µM of $ZnSO_4$ (a), and 50µM to 4000µM of $ZnSO_4$ (b). KSR1 protein was detected using α-KSR1 PA5-75208 in 1:500 dilution. N=1 (each)*

Results show that KSR1 bands were clearly expressed, including p-KSR1 bands when treated with 300µM and 500µM of $ZnSO_4$ (Figure 15.a). In figure 15.b KSR1 bands were detectable however p-KSR1 was not detected across the used concentrations of zinc. This experiment was repeated twice but it was difficult to obtain reproducible results due to the relatively low expression of KSR1 (as shown in figure 5).

## 3.3. Evaluation of KSR1 inhibitors

The results obtained in Chapter 1 revealed the effect of the zinc induced phosphorylation on KSR1 and the resulting ERK 1/2 activity. The loss of zinc in prostate cancer cells may lead to a loss of KSR1 phosphorylation (induced by zinc) that seems to contribute to cancer progression. Therefore, inhibiting KSR1 activity in prostate cancer cells may reduce its

proliferation and this resulted in the aim to develop KSR1 inhibitors. This prompted us to set up an assay to screen for KSR1 inhibitors by analysing ERK 1/2 activation, for that we used known MEK 1/2 and KSR1 inhibitors to establish the assay.

### 3.3.1. Optimisation of an assay to develop KSR1 inhibitors

The DU-145 cells showed interesting results, still we opted to use the K1-4 cell line for the KSR1 inhibitors assay because it allows expression of increased KSR1 levels leading to an enhanced ERK 1/2 activation and a higher availability of the target protein; thus, a better ability to screen for 10 new compounds based on an in-silico screen for potential KSR1 inhibitors received by the our group for further experiments. This led to a process of optimization of the techniques used with this cell line.

### 3.3.2. Optimisation of tetracycline concentration and exposure time for optimal KSR1 expression

Tetracycline induction of K1-4 cells was studied to determine the optimal concentration/expression ratio. Concentrations of 1µg/ml, 0,5µg/ml, 0,25µg/ml and 0,1µg/ml were used over a period of 1 and 2 days. Cells were plated in 12-wells plate and allowed to grow overnight, after that 4 samples were treated with Tetracycline in the concentrations mentioned above for the 2 days exposure and incubated overnight, in the following day 4 samples were treated with Tetracycline with the same concentrations for 1 day exposure and incubated overnight prior to cell lysis. After overnight incubation cells were lysed with TLB+PI; the lysates were resolved by SDS-PAGE in a 7,5% gel and analysed by Western Blot.

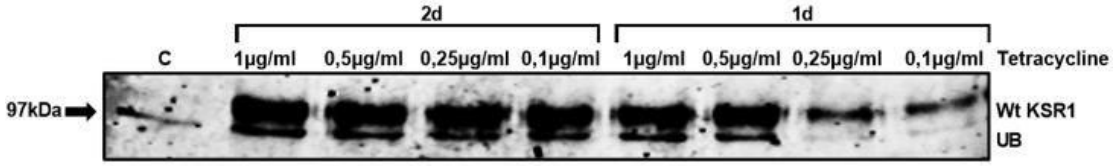


*Figure 16. Western Blot analysis of Tetracycline induced KSR1 expression under a range of concentrations of 1µg/ml to 0,1µg/ml after 1 and 2 days. The glu-glu epitope tagged KSR1 protein was detected using α-Glu-Glu tag ab18585 in 1:1000 concentration. N=1*

Results showed a similar expression between all the cells induced with tetracycline for 2 days and the 1µg/ml and 0,5µg/ml tetracycline induced cells for 1 day. As such, 1µg/ml of tetracycline for 1 day was chosen as the optimal concentration for following experiments. The primary antibody used binds to the Glu-Glu tag present in the plasmid expressed KSR1 after Tetracycline induction, the Control cells were not induced therefore it not presents the KSR1 band contrarily to what is seen in all the Tetracyline induced cells.
However, a non specific band (UB) is present in the Control and all the treated cells with a very similar strengh except in the 0,25µg/ml and 0,1µg/ml Tetracycline treated cells. This

became relevant because it seems to act as a loading control and it helped to understand that the weaker Wt KSR1 bands in the 0,25µg/ml and 0,1µg/ml Tetracycline cells probably result from a loading error instead of the effect of the concentrations of Tetracyline used in the cells.

### 3.3.3. Optimisation of assay conditions to detect ERK1/2 activation

As mentioned in section 1.6, the aim of the assay is to test the inhibitors by analysing ERK 1/2 activation and inhibition. However due to the limited amounts of the novel inhibitors available it was necessary to reduce the samples size.
We started the optimization process using the 12-Wells plate (since we knew from the previous experiments that it is a suitable size to test the cells), and 96-wells plate (to reduce the sample size and assess if the results were viable and consistent) to analyse ERK 1/2 and p-ERK 1/2 after Tetracycline and EGF treatments in K1-4 cells before testing the known MEK 1/2 and KSR1 inhibitors.

As such, K1-4 cells were plated in 12-Wells and 96-Wells plates and incubated overnight, then cells were treated with 1µg/ml of Tetracycline for 16 hours and with EGF for 30 minutes (as performed in Figure 13.a) in both 12 and 96 wells plates. Cells were lysed with TLB+PI and the lysates were resolved by SDS-PAGE in 10% gel and analysed by Wester Blot.

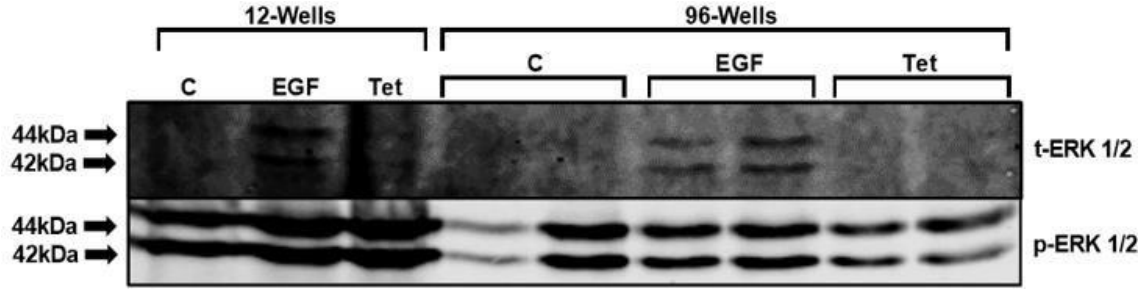


*Figure 17. Western blot analysis of t-ERK 1/2 and p-ERK 1/2 in 12-Wells plate and 96-Wells plate after exposure to EGF and Tetracycline. ERK 1/2 and p-ERK 1/2 proteins were detected using α-t-ERK 1/2 Rabbit 91025 and α-p-ERK 1/2 Mouse 91065 antibodies with a concentration of 1:5000. N=1*

Figure 17 demonstrates clear bands of p-ERK 1/2 in both 12-Wells and 96-Wells plate cells with a stronger expression in the 12-Wells cells due to the higher concentration of the protein. Contrarily to previous experiments, t-ERK 1/2 bands are only observable on the EGF treated cells.
In the 12-Wells cells the enhanced phosphorylation of ERK 1/2 by EGF and Tetracycline induction is noticeable when compared to the Control, this effect of Tetracycline alone contradicts the previous experiment (Figure 16). In the 96-Wells, the Control bands present an abnormality that may result from handling error, still the EGF and Tetracycline treated cells present the same pattern of expression as the 12-Wells cells, thus confirming the viability of 96-wells plate size for ERK 1/2 experiments.
To assure the consistency of the results previously obtained and to evaluate the effect of EGF+Tetracycline on ERK 1/2 activity and KSR1 phosphorylation after Tetracyline and

EGF induction, K1-4 cells were plated in 96-wells plate and allowed to grow overnight until 70% confluence; cells were then treated with 1µg/ml of Tetracycline and incubated overnight, in the following day cells were treated with EGF for 30 minutes as depicted in Figure 18.a, cells were lysed in TLB+PI and lysates were resolved by an 10% gel and analysed by Western Blot. The membrane was cutted horizontally in half to separate the ERK 1/2 proteins from KSR1 proteins to allow incubation with the respective specific antibodies.

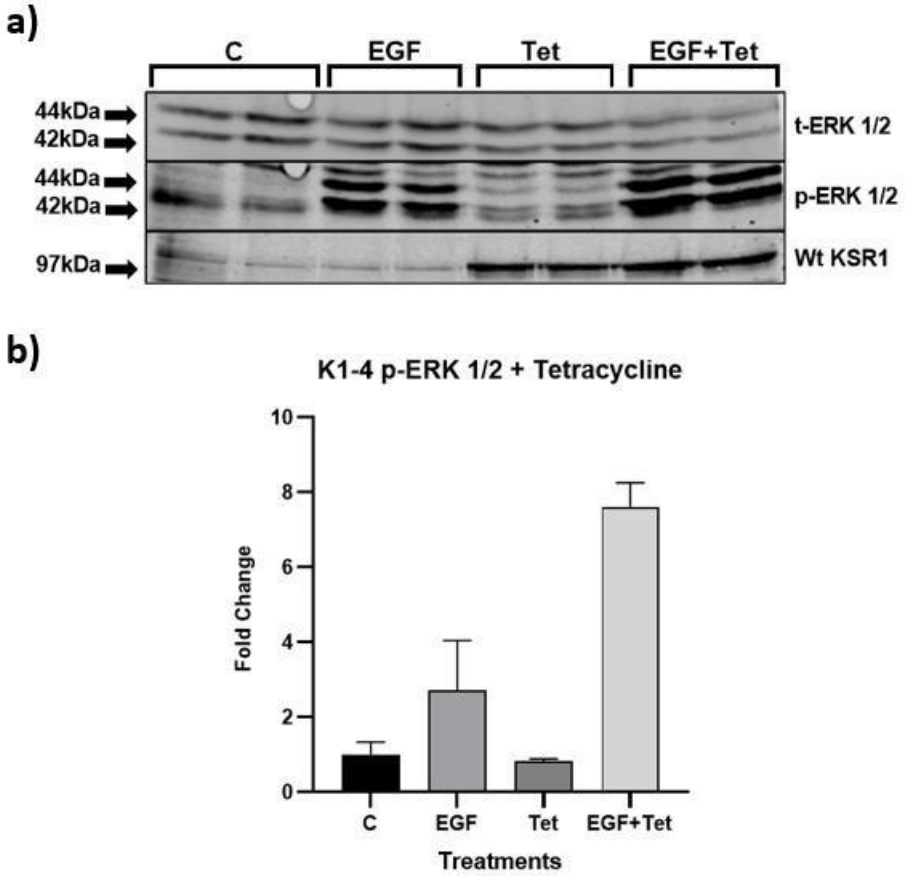


*Figure 18. Western blot analysis of t-ERK 1/2 and p-ERK 1/2 in 96-Wells plate after exposure to EGF, Tetracycline and EGF+Tetracycline. a) t-ERK 1/2, p-ERK 1/2 and KSR1 bands after exposure of K1-4 cells to EGF, Tetracycline and EGF+Tetracycline; b) Fold change in ERK 1/2 phosphorylation after cells exposure to EGF, Tetracycline and EGF+Tetracycline. Data obtained by densitometry and normalised to the Control (C) cells. Means + Standard deviation. ERK 1/2 and p-ERK 1/2 proteins were detected using α-t-ERK 1/2 Rabbit 91025 and α-p-ERK 1/2 Mouse 91065 antibodies with a concentration of 1:5000 and 1:10000 respectively, and KSR1 protein was detected using α-KSR1 PA5-75208 in 1:500 dilution. N=1*

Results exhibit identical Total ERK 1/2 (t-ERK 1/2 ) bands and strongly expressed EGF induced ERK 1/2 phosphorylated (p-ERK 1/2) bands (EGF and EGF+Tet); in addition it is visible the Tetracycline induced KSR1 bands (Tet and EGF+Tet), this demonstrates the effectiveness of tetracycline in KSR1 overexpression (Wt KSR1) (Figure 18.a).
While EGF promotes p-ERK 1/2 expression of 2.7 times higher than control (SEM±1.145), the combination of EGF+Tetracycline increases ERK 1/2 phosphorylation to more than 7 times higher than control (SEM±1.87) due to the enhancement by increased KSR1 levels

(Figure 18.b). Nevertheless, the serum-starved cells treated only with Tetracycline (Tet) express low levels of p-ERK 1/2 (Figures 18.a and 18.b) despite high levels of KSR1.

### 3.3.4. Evaluation of MEK and KSR1 inhibitors on ERK 1/2 activity

In order to understand the effect of potential KSR1 inhibitors on ERK 1/2 activity, we opted to test K1-4 cells with the only commercially available KSR1 inhibitor APS-2-79 (concentrations of 5µM, 10µM, 20µM, and 50µM) and with the well-described MEK 1/2 inhibitor PD184352 as a positive control of ERK 1/2 inhibition (concentrations of 1µM, 2.5µM, 5µM, 10µM and 20µM). The inhibitors were diluted in DMSO upon preparation from lyophilised stock, due to this DMSO (final dilution of 1:200) was added to the EGF treated cells to provide the same experimental conditions.
Cells were seeded in 96-well plate and allowed to grow until 70% confluency following serum starving overnight. In the following day, cells were treated with APS-2-79 KSR and PD184352 MEK 1/2 inhibitors for 2 hours at concentrations described above, and EGF for 30 minutes as depicted in Figure 19. Cells were lysed in TLB+PI and lysates were resolved by SDS-PAGE in 10% Gel and analysed by Western Blot.

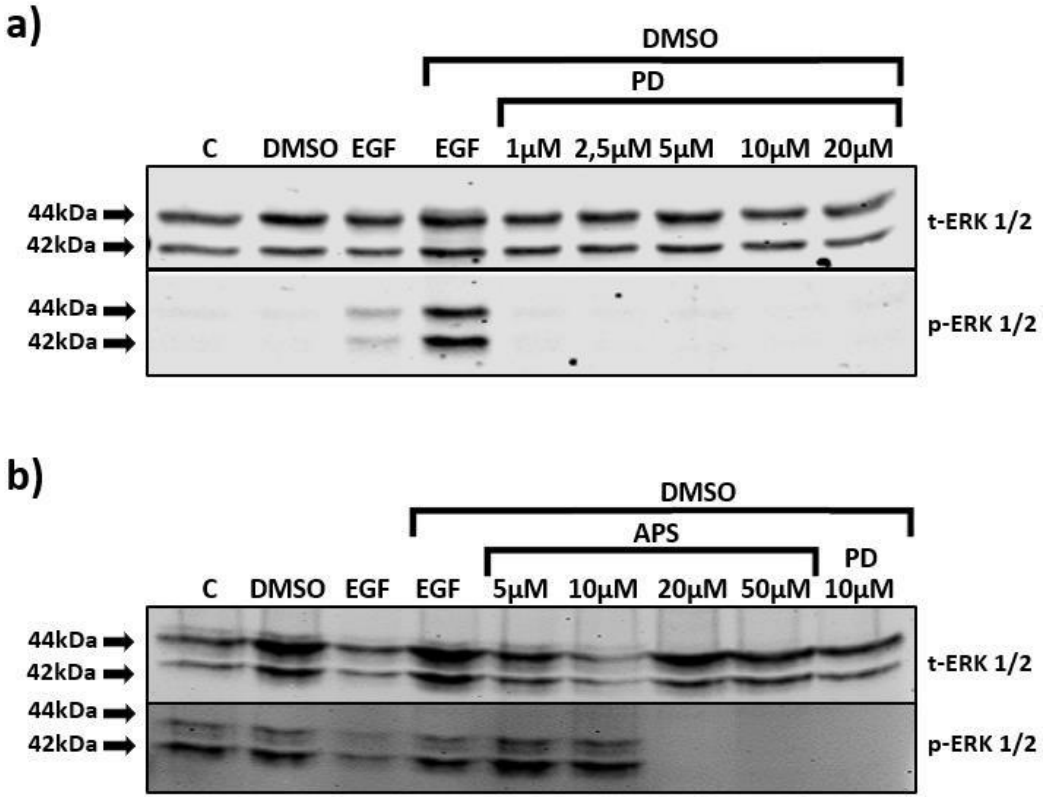


*Figure 19. Western blot analysis of t-ERK 1/2 and p-ERK 1/2 in 96-Wells plate after exposure to EGF and PD184352 (1µM, 2.5µM, 5µM, 10µM and 20µM) (a) and EGF and APS-2-79 (5µM, 10µM, 20µM and 50µM) (b) with a positive control treated with PD184352 (10µM). ERK 1/2 and p-ERK 1/2 proteins were detected using α-t-ERK 1/2 Rabbit 91025 and α-p-ERK 1/2 Mouse 91065 antibodies with a concentration of 1:5000 and 1:10000 respectively. N=2*

The results demonstrate an effective inhibition of ERK 1/2 phosphorylation by PD184352 (Figure 19.a) across all concentrations. The Control and DMSO cells did not present phosphorylated bands since not stimulation treatment was applied, contrarily to this, EGF and EGF + DMSO treated cells exhibited p-ERK 1/2 bands, with the EGF+DMSO treated cells demonstrating a stronger signal. These results allow the observation of the activation of ERK 1/2 upon EGF stimulation and consequently inhibition by PD184352, thus indicating this inhibitor as a positive control for inhibition of this pathway.

Figure 19.b shows the results of the cells exposure to the APS-2-79 KSR inhibitor, with an efficient inhibitory effect when 20µM and 50µM concentrations were used. Conversely with the results in Figure 19.a, EGF and EGF+DMSO treated cells presented p-ERK 1/2 bands indicating the activation of ERK 1/2 proteins. However, contrarily to the PD184352 treatments experiment, Control and DMSO treated cells also presented p-ERK 1/2 bands, suggesting that the cells were not efficiently starved. Nevertheless, both inhibitors showed the ability to successfully inhibit ERK 1/2 activity.

### 3.3.5. Live-cell analysis of cell growth after treatment with MEK1/2 and KSR1 inhibitors

The ability of the inhibitors to reduce cell growth to validate the previous assay was studied by using PD184352 MEK 1/2 and APS-2-79 KSR inhibitors (concentrations in a range of 1µM, 5µM and 10µM) to inhibit these proteins and compare cell growth by analysing the cell confluence evolution with a non-treated cells (C). As in the previous experiment, the inhibitors were diluted in DMSO therefore DMSO (final dilution of 1:200) was again added to the EGF treated cells to provide the same conditions. Cells were seeded in 96-wells, treated with the inhibitors individually and placed in the Muvicyte™ live cell imager inside an incubator over a time course of 65h and cell confluence was measured every 5 hours by the MuviCyte™ live-cell imaging kit.

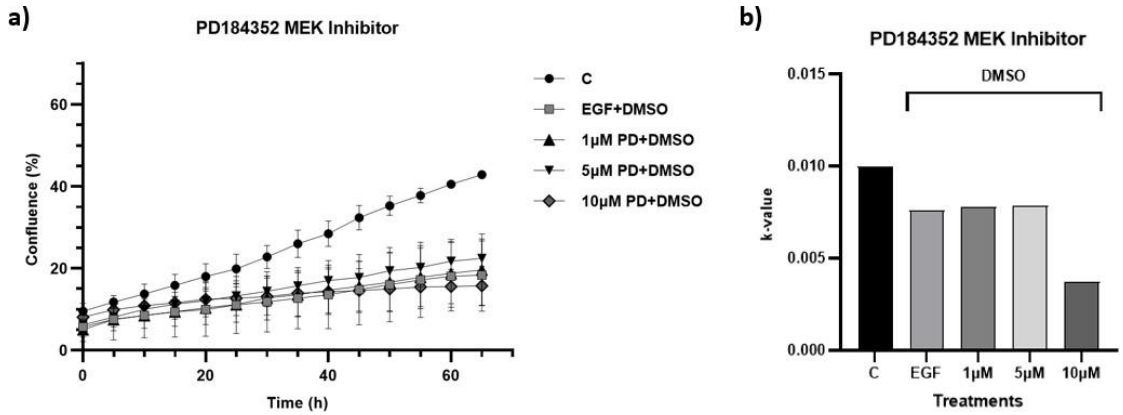


*Figure 20. Cell confluence evolution (in percentage) over 65 hours with PD184352 MEK inhibitor treatment on K1-4 cells (a) and calculated k-value from linear regression equation of logarithmic confluence values (b); Cell confluence values obtained by MuviCyte™ live-cell imaging kit. N=1*

Cells that were subjected to the treatment showed a difference in growth rate compared to the control (Figure 20.a). Nonetheless, the treatment with 10µM PD184352 MEK 1/2 was shown to exhibit the highest inhibitory effect (Figure 20.b).
presents the k-value (slope) of each curve demonstrating a contrasting higher growth rate of Control and that 10µM PD184352 MEK 1/2 inhibits cell growth in the assay. C, EGF, 1µM and 5µM PD184352-treated cells show similar slopes meaning identical growth rates with no identifiable effect of PD184352 MEK 1/2 Inhibitor at used concentrations.

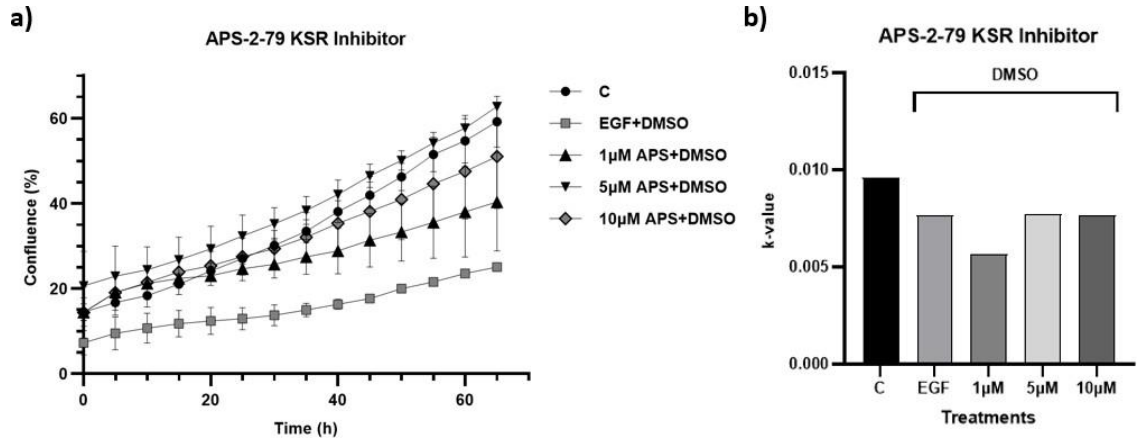


*Figure 21. Cell confluence evolution (in percentage) over 65 hours with APS-2-79 KSR inhibitor treatment on K1-4 cells (a) and calculated k-value from linear regression equation of logarithmic confluence values (b); Cell confluence values obtained by MuviCyte™ live-cell imaging kit. N=1*

The APS-2-79 KSR Inhibitor experiment did not show a significant difference in the growth of the cells between the inhibitor concentrations. Similarly, to the PD184352 MEK 1/2 experiment, it is visible an enhanced growth of the Control cells compared to the DMSO co-treated cells.
Also, DMSO co-treated cells (EGF, 5µM and 10µM) present similar slopes apart from 1µM APS-2-79 treated cells.

# 4. Discussion

## 4.1. Zinc induces phosphorylation of KSR1 in the prostate cancer cell lines DU-145 and PC-3

The hypothesis of this study as mentioned in section 1.6 is that the Zinc induces KSR1 phosphorylation in prostate cancer cells, resulting in decreased ERK 1/2 activity.
Zinc is known to induce phosphorylation in several proteins including in the MAPK-ERK pathway, however Zinc induced KSR1 phosphorylation was only described in the model organism Caenorhabditis elegans. In fact, KSR1 is poorly described in the classical Prostate cancer cell lines DU-145, PC-3 and LNCaP. It is also known that different cell lines have

diverse expression levels for the same protein but a direct comparison of KSR1 expression between these three cell lines is not described yet.
Figure 5 clearly shows the variation of KSR1 expression between the three cell lines, with a much higher expression in LNCaP compared to DU-145 cells and a non-detectable expression in PC-3 cells, this corroborates previous experiments performed in the laboratory (data not shown) and follows the same pattern of Androgen Receptors expression levels (highly expressed in LNCaP, detectable in DU-145 and barely to not detectable in PC-3) of these cell lines [58]. This might mean a connection between androgen receptors, KSR1 expression and the MAPK-ERK pathway activity with androgen stimulation of cancer cells being able to influence KSR1 levels, as seen in the lower KSR1 expression in DU-145 compared to LNCaP cells, and non-detectable levels in PC-3.

Thus DU-145 cell line, as explained in section 3.1.1, fit the purpose of optimal cell line for the Zinc induced phosphorylation of KSR1 assay. Nonetheless, cells were transfected with pcDNA3-mKSR1 plasmid for enhanced expression of KSR1 – with the intent of granting better results in the assay – and its efficiency assessed by comparison with K1-4 transfected cells. DU-145 cells are notoriously difficult to transfect, as shown in Figure 6, however the Viafect Reagent presents more efficiency in transfecting DU-145 cells than other techniques used (data not shown). While DU-145 cells transfection was less than K1-4 cells, it was a good result for this cell line and enough to affect assays results as shown in Figures 8.a and 9.c, where zinc induction of KSR1 phosphorylation is only detectable in transfected cells, indicating that the p-KSR1 levels in Wt DU-145 are below detection level or/and the existence of a different interaction between zinc and the exogenous KSR1 expressed by the pcDNA3-mKSR1 that results in its increased phosphorylation, hence detectable by immunoblotting.

Interestingly, the KSR1 phosphorylation levels obtained in this assay demonstrate an incomplete phosphorylation of total KRS1 protein as opposed to what was demonstrated by Yoder et al [46]; this can be explained by the loss of zinc transporters in Prostate cancer cells causing a reduced uptake of $ZnSO_4$ to the cell hence the diminished phosphorylating effect on KSR1. This can also be deduced by the increased p-KSR1 when the cells are stimulated with higher concentrations of $ZnSO_4$, suggesting that if more zinc can enter the cell, it will induce a more effective phosphorylation.

The approach chosen to tackle the limitation of the loss of Zinc transporters by the Prostate cancer cell line DU-145 was to increase zinc permeability by using the Zinc Ionophore Mercaptopyridine. Zinc can be toxic to cells in very elevated concentrations, however as seen in Figure 11, the concentrations used did not induce cell death. The use of Mercaptopyridine combined with $ZnSO_4$ seems to decrease cell resistance to Zinc toxicity since more than 5µM of $ZnSO_4$ resulted in cell death (Figure 10). All the cells that underwent the treatment with non-lethal concentrations failed to present p-KSR1 bands (Figure 11) implying that zinc concentrations used, even with high periods of exposure (6 and 9 hours), were insufficient to induce KSR1 phosphorylation in DU-145 cells. The use of Mercaptopyridine can be useful for increasing intracellular zinc and overcome the loss of zinc transporters but in opposition to the latter, Mercaptopyridine is an ionophore, therefore unregulated which can lead to the toxicity problems. An alternative approach like inducing the expression of Zinc transporters like the ZIP1 (which occurs naturally in normal prostate

cells) might help tackling this problem and allow a better understanding of the effects of Zinc in KSR1 phosphorylation in prostate cancer cells.

The same initial approach to evaluate Zinc induced phosphorylation of KSR1 in DU-145 cells was performed in the PC-3 cell line. This cell line, as described above, exhibits very low KSR1 protein levels which caused difficulties in achieving clean results (data not shown) due to the presence of non-specific bands and background. Despite that, we managed to obtain the results of $ZnSO_4$ treatments in Wt PC-3 cells, and phosphorylated bands were detected in the 300µM and 500µM treated cells (Figure 15.a). Regardless of the low levels of KSR1 expressed by PC-3 cells, it was possible to observe Zinc induced phosphorylation in Wt PC-3 cells, which did not occur with the DU-145 cells, this might be due to this cell line expressing more Zinc transporters than DU-145 cells which allows it to accumulate higher levels of Zinc [59].

Due to the results obtained in Figure 15.c where those bands were not visible, the Zinc induced phosphorylation of KSR1 in Wt cells presents a variability that requires repeating the assay and further experiments to confirm the results, such as transfection with a KSR1 plasmid to access Zinc induced phosphorylation.

## 4.2. Zinc modulates ERK 1/2 activity in Transfected DU-145 cells

We proposed to investigate the activity of ERK1/2 in transfected DU-145 cells under exposure to $ZnSO_4$ and EGF to assess its effect on the cells with enhanced levels of KSR1 and how this interaction modulates ERK 1/2 activity.

As depicted in Figure 13, notable differences were observed between the starved and non-starved cells, where the presence or absence of serum in the media played a significant role. Fetal bovine serum (FBS), contains various growth factors that activate receptor tyrosine kinases (RTKs), thereby initiating the MAPK/ERK pathway. Consequently, measurable levels of constitutive ERK 1/2 phosphorylation occurs, making it challenging to obtain accurate results from treatments involving growth factors such as EGF due to receptor saturation.

Non-starved cells present similar p-ERK bands indicating serum stimulation of ERK 1/2 (Figure 13.a), but in the Starved cells, when the ERK 1/2 activity is at basal levels, EGF induces ERK 1/2 phosphorylation to more than 10 times compared to Control confirming the high stimulating capacity of EGF as described by Martin-Vega et al. thus revealing the relevance of starving the cells prior to experiments for accurate results.

Another aim of this assay was to investigate how the Zinc-induced phosphorylation of KSR1 affects ERK 1/2 to evaluate if KSR1 phosphorylation results in reduced ERK 1/2 activity and the importance of Zinc in this relation.

KSR1+$ZnSO_4$ treated cells in full media shows a small increase of ERK 1/2 phosphorylation (Figure 13.b) similar to the homologous Starved cells, which might be due to the Zinc ability to induce phosphorylation. This can be deduced by comparing the Zinc treated Starved

(KSR1+$ZnSO_4$) cells with both KSR1 Starved cells (KSR1) and the GFP control where no treatment was applied and therefore ERK 1/2 was not stimulated, hence no activity detected.

Contrarily to the assay above, Figure 14 shows that while EGF treatment results in an elevated level of p-ERK 1/2, the $ZnSO_4$ treated cells exhibit bands with p-ERK 1/2 levels below the Control cells (CT) and similar to the non-transfected control cells (CU), this variation of results between assays might be due to the experiments being performed once for screening or an error during the experiment, therefore replicates are required to assure results.

## 4.3. K1-4 cell growth is reduced by MEK and KSR inhibitors

The results obtained in Chapter 1 suggest that Zinc induced phosphorylation of KSR1 might reduce ERK 1/2 phosphorylation, thus reducing the MAPK-ERK pathway activity resulting in diminished transcription of cell proliferation and survival genes.
A successful negative effect of these inhibitors in K1-4 cell growth is a crucial step in the development of an assay with KSR1 inhibitors towards a more efficient KSR1 inhibition and consequent reduced prostate cancer cell proliferation. To do that we developed an optimization process for the assay that relied on obtaining consistent results when decreasing the cell culture plate size, and further live-analysis of cell growth under exposure to the inhibitors, with all the results detailed in Section 3.3.5.

### 4.3.1. Optimization process for K1-4 assays

The experiments represented in Figure 17 and Figure 18 had the main purpose of testing if whether or not the assay would be reliable and reproducible in the 96-Wells plate. The results allowed us to opt for the 96-Wells plate to proceed with the assay, however the results indicated inconsistency between plates and between duplicates; in addition, the results obtained in both experiments showed a variation for the same treatments, thus requiring the replication of this experiment in the future.

Regarding the Control cells, in Figure 17, there is a clear difference in expression levels of p-ERK 1/2, as seen in Figure 13 regarding Prostate Cancer cells, the use of starved media should deplete the receptors of most binding molecules resulting in a low expression band, that is seen the one of the replicates of the Control cells of the 96-Wells plate and also seen in Figure 17, however the Control of the 12-Wells plate present a strong band similar to the band obtained in the other replicate of the 96-Wells plate that might be caused by a possible mistake during the experiment.

The cells treated with tetracycline to induce KSR1 expression showed consistency in Figure 17 but diverged from the results obtained in Figure 18. It was expected that the elevated levels of KSR1 would induce phosphorylation of ERK 1/2 as seen in Figure 17 in both plates, with and without EGF stimulation. Notwithstanding, the elevated levels of KSR1 might disaggregate the signalling complex describe in Figure 4 and therefore is not capable of inducing the phosphorylation of ERK 1/2 resulting in very low levels of p-ERK 1/2 which

could explain the results in Figure 18 since the p-ERK 1/2 bands are weaker than the Control bands. Even though the same concentration of Tetracycline was used to induce KSR1 overexpression in both experiments, it is not possible to confirm equal levels of KSR1 between experiments and it is also not clear the exact KSR1 concentration needed to cross the threshold of elevated ERK 1/2 phosphorylation to the signalling complex disaggregation (see section 1.4).

EGF strongly activates the MAPK-ERK pathway leading to ERK 1/2 phosphorylation, the results of EGF treatment demonstrated similarities between the experiments with p-ERK 1/2 levels higher than the Control. The Tetracycline induction combined to EGF stimulation amplifies the activation of the MAPK-ERK pathway, this results in enhanced expression of KSR1 which along with the EGF stimulation enhances the signalling cascade, hence ERK 1/2 activation. This leads to in strongly expressed bands of p-ERK 1/2 (Figure 18) with levels almost eight times more elevated than the control, thus highlighting the relation between growth factor stimulation and KSR1 regulation of the signalling pathway. The results of this assay permitted to define the optimal conditions for future K1-4 assays, with the cell induction with Tetracycline and EGF stimulation for enhanced KSR1 expression and ERK 1/2 activation, which should allow clearer results.

## 4.4. ERK 1/2 activation is inhibited by MEK and KSR inhibitors

PD184352 MEK is known for its ability to inhibit more than 90% of ERK 1/2 and it was described to reduce cell growth in several cell lines including cancer cell lines. Due to its efficiency in inhibiting ERK 1/2 activation, PD184352 MEK was used as a positive control to test the efficacy of the KSR inhibitor APS-2-79 to reduce ERK 1/2 activation.

The results in Figure 19.a confirmed the PD184352 inhibitory ability towards ERK 1/2 at all the concentrations tested. Finally, 10µM was chosen as an optimal concentration for the positive control in further experiments, as the Figure 19.b demonstrates.
Although p-ERK 1/2 was detected in the control when testing APS-2-79, the ability of the latter to reduce ERK 1/2 activation at 20µM and 50µM was comparable to 10 µM PD(Figure 19.b). As described in section 1.3.2, high levels of APS-2-79 can become cytotoxic, evidencing the need of the development of a more effective inhibitor that can successfully affect the MAPK/ERK 1/2 pathway at a lower concentration.

Optimisations are still required to ensure basal levels of ERK 1/2 activation upon Serum-starvation. Nevertheless, the results obtained are promising for the use of APS-2-79 on the assessment of new KSR1 inhibitors effect on ERK 1/2 phosphorylation.

## 4.5. Live-analysis of MEK and KSR inhibitors on cell growth

The results seen in Figure 20 suggest an inhibitory effect of the MEK inhibitor in cell growth when compared to the control, the cells treated with 10µM PD + DMSO showed a lower k-

value than the other cells, meaning a slower growth with this concentration of the MEK Inhibitor, still all the other treated cells (1µM and 5µM +DMSO) present a less reduced growth compared to the 10µM treated cells but also a slower growth compared to the control cells. However, the EGF+DMSO treated cells shows a very similar growth and k-value to the 1µM and 5µM PD + DMSO treated cells which might be due to a cell growth inhibitory effect of DMSO (1:200) in all cells thus preventing the assessment of sole MEK efficiency.

The screening experiment above was meaningful to assess the diminished cell growth when the MEK is inhibited, we then performed the experiment with the same concentrations of APS-2-79 KSR inhibitor and similarly to the previous experiment, all the DMSO treated cells showed a slower growth compared to the control suggesting the DMSO cell growth inhibitory effect (Figure 21). Replicates and further experiments with increased concentrations of these inhibitors (i.e the concentrations used in Figure 19.b) are required for more accurate results.

# 5. Conclusion

The results obtained in this study met the proposed hypothesis and the objectives set were achieved.
The experiments performed allowed further understanding of the role of Zinc in the MAPK/ERK pathway, its inhibitory effect on KSR1 and how KSR1 regulates ERK 1/2 activity.
It was also observed how the loss of Zinc transporters in prostate cancer cells diminished the Zinc induction of KSR1 phosphorylation. Nevertheless, the objectives were achieved by demonstrating that inhibition of KSR1 results in diminished ERK 1/2 activity.
However, it is clear that it is necessary to mimic Zinc inhibitory effect on KSR1 through the development of new KSR1 inhibitors to tackle prostate cancer cells proliferation.
Further studies on the uptake of zinc by prostate cancer cells need to be performed to understand more about the same level of KSR1 effect on normal and prostate cancer cells.
Also, a better approach to the assessment of the MEK and KSR1 inhibitors effect on cell growth is required to understand how cells behave on a long period. The results of the enhanced KSR1 expression derived from Tetracycline induction presents an interesting future study to evaluate the efficacy of new KSR1 inhibitors.
Finally, as mentioned in section 4.5, it is necessary to develop effective KSR1 inhibitors to successfully cease ERK 1/2 activity in prostate cancer cells, hence reducing its proliferation.

# 6. References


1. Barsouk, A. *et al.* Epidemiology, Staging and Management of Prostate Cancer. *Medical Sciences 2020, Vol. 8, Page 28* **8**, 28 (2020).
2. Dunn, M. W. & Kazer, M. W. Prostate Cancer Overview. *Semin Oncol Nurs* **27**, 241–250 (2011).
3. Rebello, R. J. *et al.* Prostate cancer. *Nature Reviews Disease Primers 2021 7:1* **7**, 1–27 (2021).
4. Lee, C. H., Akin-Olugbade, O. & Kirschenbaum, A. Overview of Prostate Anatomy, Histology, and Pathology. *Endocrinol Metab Clin North Am* **40**, 565–575 (2011).
5. Dunn, M. W. Prostate Cancer Screening. *Semin Oncol Nurs* **33**, 156–164 (2017).
6. Fitzgerald, R. C. Pre-invasive disease: Pathogenesis and clinical management. *Pre-Invasive Disease: Pathogenesis and Clinical Management* 1–519 (2011) doi:10.1007/978-1-4419-6694-0/COVER.
7. Miah, S. & Catto, J. BPH and prostate cancer risk. *Indian J Urol* **30**, 214 (2014).
8. Kwon, O. J., Zhang, L., Ittmann, M. M. & Xin, L. Prostatic inflammation enhances basal-to-luminal differentiation and accelerates initiation of prostate cancer with a basal cell origin. *Proc Natl Acad Sci U S A* **111**, E592–E600 (2014).
9. Liu, A. Y. & True, L. D. Characterization of Prostate Cell Types by CD Cell Surface Molecules. *Am J Pathol* **160**, 37 (2002).
10. Global Cancer Observatory. https://gco.iarc.fr/.
11. Hussein, S., Satturwar, S. & Van Der Kwast, T. Young-age prostate cancer. *J Clin Pathol* **68**, 511–515 (2015).
12. Rawla, P. Epidemiology of Prostate Cancer. *World J Oncol* **10**, 63 (2019).
13. Wadosky, K. M. & Koochekpour, S. Therapeutic Rationales, Progresses, Failures, and Future Directions for Advanced Prostate Cancer. *Int J Biol Sci* **12**, 409 (2016).
14. Gomez, L., Kovac, J. R. & Lamb, D. J. CYP17A1 inhibitors in castration-resistant prostate cancer. *Steroids* **95**, 80–87 (2015).
15. Saxena, P. *et al.* PSA regulates androgen receptor expression in prostate cancer cells. *Prostate* **72**, 769–776 (2012).
16. Matuszak, E. A. & Kyprianou, N. Androgen regulation of epithelial–mesenchymal transition in prostate tumorigenesis. *http://dx.doi.org/10.1586/eem.11.32* **6**, 469–482 (2014).
17. Taichman, R. S., Loberg, R. D., Mehra, R. & Pienta, K. J. The evolving biology and treatment of prostate cancer. *Journal of Clinical Investigation* **117**, 2351–2361 (2007).
18. Gioeli, D., Mandel, J. W., Petroni, G. R., Frierson, H. F. & Weber, M. J. Activation of Mitogen-Activated Protein Kinase Associated with Prostate Cancer Progression1 | Cancer Research | American Association for Cancer Research. *Cancer Res* **59**, 279–284 (1999).
19. Weir, E. G., Partin, A. W. & Epstein, J. I. CORRELATION OF SERUM PROSTATE SPECIFIC ANTIGEN AND QUANTITATIVE IMMUNOHISTOCHEMISTRY. *J Urol* **163**, 1739–1742 (2000).
20. Saini, S. PSA and beyond: alternative prostate cancer biomarkers. *Cellular Oncology* **39**, 97–106 (2016).
21. Litwin, M. S. & Tan, H. J. The Diagnosis and Treatment of Prostate Cancer: A Review. *JAMA* **317**, 2532–2542 (2017).
22. Descotes, J. L. Diagnosis of prostate cancer. *Asian J Urol* **6**, 129–136 (2019).
23. Hoffman, R. M. Clinical practice. Screening for prostate cancer. *N Engl J Med* **365**, 2013–9 (2011).
24. Teo, M. Y., Rathkopf, D. E. & Kantoff, P. Treatment of Advanced Prostate Cancer. *https://doi.org/10.1146/annurev-med-051517-011947* **70**, 479–499 (2019).
25. Wang, G., Zhao, D., Spring, D. J. & Depinho, R. A. Genetics and biology of prostate cancer. *Genes Dev* **32**, 1105 (2018).
26. Locally advanced prostate cancer | Cancer Research UK. https://www.cancerresearchuk.org/about-cancer/prostate-cancer/stages/locally-advanced-prostate-cancer.
27. Okpua, N. C., Okekpa, S. I., Njaka, S. & Emeh, A. N. Clinical diagnosis of prostate cancer using digital rectal examination and prostate-specific antigen tests: a systematic review and meta-analysis of sensitivity and specificity. *African Journal of Urology* **27**, 1–9 (2021).
28. Sajjad, W. *et al.* Diagnostic value of the abnormal digital rectal examination in the modern MRI-based prostate cancer diagnostic pathway. *J Clin Urol* (2022) doi:10.1177/20514158221091402/SUPPL_FILE/SJ-DOCX-1-URO-10.1177_20514158221091402.DOCX.

29. Halpern, J. A. *et al.* Utility of Digital Rectal Examination (DRE) as an Adjunct to Prostate Specific Antigen (PSA) in the Detection of Clinically Significant Prostate Cancer. *J Urol* **199**, 947 (2018).
30. Guo, Y. *et al.* ERK/MAPK signalling pathway and tumorigenesis (Review). *Exp Ther Med* **19**, 1997–2007 (2020).
31. Kim, E. K. & Choi, E. J. Pathological roles of MAPK signaling pathways in human diseases. *Biochimica et Biophysica Acta (BBA) - Molecular Basis of Disease* **1802**, 396–405 (2010).
32. Cargnello, M. & Roux, P. P. Activation and Function of the MAPKs and Their Substrates, the MAPK-Activated Protein Kinases. *Microbiology and Molecular Biology Reviews* **75**, 50–83 (2011).
33. Kabir, M. H., Patrick, R., Ho, J. W. K. & O'Connor, M. D. Identification of active signaling pathways by integrating gene expression and protein interaction data. *BMC Syst Biol* **12**, 77–87 (2018).
34. Dougherty, M. K. *et al.* Regulation of Raf-1 by direct feedback phosphorylation. *Mol Cell* **17**, 215–224 (2005).
35. Lake, D., Corrêa, S. A. L. & Müller, J. Negative feedback regulation of the ERK1/2 MAPK pathway. *Cellular and Molecular Life Sciences* **73**, 4397–4413 (2016).
36. Torrealba, N. *et al.* Expression of ERK1 and ERK2 in prostate cancer. *MAP Kinase* **4**, (2015).
37. Rodríguez-Berriguete, G. *et al.* MAP Kinases and Prostate Cancer. *J Signal Transduct* **2012**, 1–9 (2012).
38. Müller, J., Cacace, A. M., Lyons, W. E., McGill, C. B. & Morrison, D. K. Identification of B-KSR1, a Novel Brain-Specific Isoform of KSR1 That Functions in Neuronal Signaling. *Mol Cell Biol* **20**, 5529 (2000).
39. Llobet, D. *et al.* KSR1 Is Overexpressed in Endometrial Carcinoma and Regulates Proliferation and TRAIL-Induced Apoptosis by Modulating FLIP Levels. *Am J Pathol* **178**, 1529–1543 (2011).
40. Zhou, M., Horita, D. A., Waugh, D. S., Byrd, R. A. & Morrison, D. K. Solution structure and functional analysis of the cysteine-rich C1 domain of kinase suppressor of ras (KSR). *J Mol Biol* **315**, 435–446 (2002).
41. Paniagua, G. *et al.* KSR induces RAS-independent MAPK pathway activation and modulates the efficacy of KRAS inhibitors. *Mol Oncol* (2022) doi:10.1002/1878-0261.13213.
42. Müller, J., Ory, S., Copeland, T., Piwnica-Worms, H. & Morrison, D. K. C-TAK1 Regulates Ras Signaling by Phosphorylating the MAPK Scaffold, KSR1. *Mol Cell* **8**, 983–993 (2001).
43. Zhang, H., Koo, C. Y., Stebbing, J. & Giamas, G. The dual function of KSR1: a pseudokinase and beyond. *Biochem Soc Trans* **41**, 1078–1082 (2013).
44. Mckay, M. M., Freeman, A. K. & Morrison, D. K. Complexity in KSR function revealed by Raf inhibitor and KSR structure studies. *Small GTPases* **2**, 276 (2011).
45. Neilsen, B. K., Frodyma, D. E., Lewis, R. E. & Fisher, K. W. KSR as a therapeutic target for Ras-dependent cancers. *Expert Opin Ther Targets* **21**, 499 (2017).
46. Yoder, J. H., Chong, H., Guan, K. I. & Han, M. Modulation of KSR activity in Caenorhabditis elegans by Zn ions, PAR-1 kinase and PP2A phosphatase. *EMBO J* **23**, 111–119 (2004).
47. Zhao, Z., Zhu, L., Xing, Y. & Zhang, Z. Praja2 suppresses the growth of gastric cancer by ubiquitylation of KSR1 and inhibiting MEK-ERK signal pathways. *Aging (Albany NY)* **13**, 3886 (2021).
48. Rao, C. *et al.* KSR1-and ERK-dependent translational regulation of the epithelial-to-mesenchymal transition. doi:10.7554/eLife.
49. Canal, F., Palygin, O., Pankratov, Y., Corrêa, S. A. L. & Müller, J. Compartmentalization of the MAPK scaffold protein KSR1 modulates synaptic plasticity in hippocampal neurons. *The FASEB Journal* **25**, 2362–2372 (2011).
50. Hacioglu, C., Kacar, S., Kar, F., Kanbak, G. & Sahinturk, V. Concentration-Dependent Effects of Zinc Sulfate on DU-145 Human Prostate Cancer Cell Line: Oxidative, Apoptotic, Inflammatory, and Morphological Analyzes. *Biol Trace Elem Res* **195**, 436–444 (2020).
51. Costello, L. C. & Franklin, R. B. A comprehensive review of the role of zinc in normal prostate function and metabolism; and its implications in prostate cancer. *Arch Biochem Biophys* **611**, 100–112 (2016).
52. Costello, L. C., Franklin, R. B., Feng, P., Tan, M. & Bagasra, O. Zinc and prostate cancer: a critical scientific, medical, and public interest issue (United States). doi:10.1007/s10552-005-2367-y.
53. Costello, L. C. & Franklin, R. B. Novel Role of Zinc in the Regulation of Prostate Citrate Metabolism and Its Implications in Prostate Cancer. *Prostate* **35**, 285–296 (1998).

54. Dubi, N., Gheber, L., Fishman, D., Sekler, I. & Hershfinkel, M. Extracellular zinc and zinc-citrate, acting through a putative zinc-sensing receptor, regulate growth and survival of prostate cancer cells. *Carcinogenesis* **29**, 1692–1700 (2008).
55. Franklin, R. B. & Costello, L. C. Zinc as an anti-tumor agent in prostate cancer and in other cancers. *Arch Biochem Biophys* **463**, 211–217 (2007).
56. To, P. K., Do, M. H., Cho, J. H. & Jung, C. Growth Modulatory Role of Zinc in Prostate Cancer and Application to Cancer Therapeutics. *Int J Mol Sci* **21**, (2020).
57. Franklin, R. B. *et al.* Human ZIP1 is a major zinc uptake transporter for the accumulation of zinc in prostate cells. *J Inorg Biochem* **96**, 435–442 (2003).
58. Alimirah, F., Chen, J., Basrawala, Z., Xin, H. & Choubey, D. DU-145 and PC-3 human prostate cancer cell lines express androgen receptor: Implications for the androgen receptor functions and regulation. *FEBS Lett* **580**, 2294–2300 (2006).
59. Costellot, L. C., Liu, Y., Zou, J. & Franklin, R. B. Evidence for a zinc uptake transporter in human prostate cancer cells which is regulated by prolactin and testosterone. *Journal of Biological Chemistry* **274**, 17499–17504 (1999).